



**INVESTIGATION ON THE EFFECT OF TOOL GEOMETRY
FEATURES TO MINIMIZE DAMAGES DURING TRIMMING OF
HYBRID FIBRE REINFORCED POLYMER (HFRP) MATERIAL -
AEROSTRUCTURAL COMPONENT**



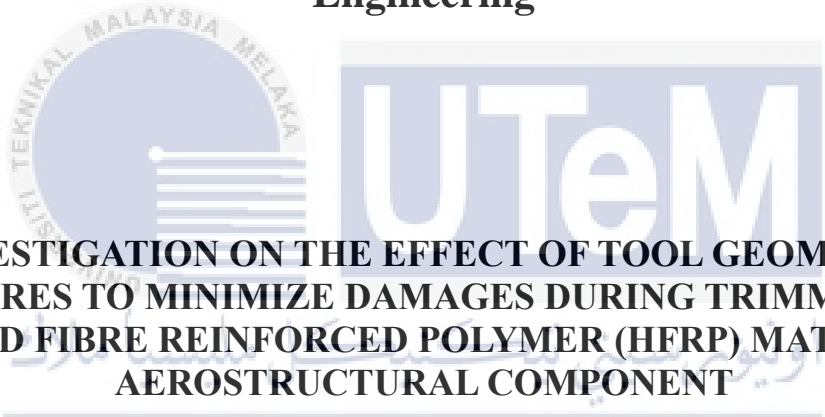
**NUR AZALINA BINTI ANUAR
B092010109**

**BACHELOR OF MANUFACTURING ENGINEERING
TECHNOLOGY (PRODUCT DESIGN) WITH HONOURS**

2024



**Faculty of Industrial and Manufacturing Technology and
Engineering**



**INVESTIGATION ON THE EFFECT OF TOOL GEOMETRY
FEATURES TO MINIMIZE DAMAGES DURING TRIMMING OF
HYBRID FIBRE REINFORCED POLYMER (HFRP) MATERIAL -
AEROSTRUCTURAL COMPONENT**

UNIVERSITI TEKNIKAL MALAYSIA MELAKA

NUR AZALINA BINTI ANUAR

Bachelor of Manufacturing Engineering Technology (Product Design) with Honours

2024

**INVESTIGATION ON THE EFFECT OF TOOL GEOMETRY FEATURES TO
MINIMIZE DAMAGES DURING TRIMMING OF HYBRID FIBRE
REINFORCED POLYMER (HFRP) MATERIAL -AEROSTRUCTURAL
COMPONENT**

NUR AZALINA BINTI ANUAR



Faculty of Mechanical and Manufacturing Engineering Technology

UNIVERSITI TEKNIKAL MALAYSIA MELAKA

2024

DECLARATION

I declare that this Choose an item. entitled “ INVESTIGATION ON THE EFFECT OF TOOL GEOMETRY FEATURES TO MINIMIZE DAMAGES DURING TRIMMING OF HYBRID FIBRE REINFORCED POLYMER (HFRP) MATERIAL - AEROSTRUCTURAL COMPONENT” is the result of my own research except as cited in the references. The Choose an item. has not been accepted for any degree and is not concurrently submitted in candidature of any other degree.



Signature

اونيورسيتي تيكنيكل مليسيا ملاك

Name

: NUR AZALINA BINTI ANUAR

Date

: 12 January 2024

APPROVAL

I hereby declare that I have checked this thesis and in my opinion, this thesis is adequate in terms of scope and quality for the award of the Bachelor of Manufacturing Engineering Technology (Product Design) with Honours.

Signature :



Supervisor Name : Ts. Dr. Syahrul Azwan bin Sundi

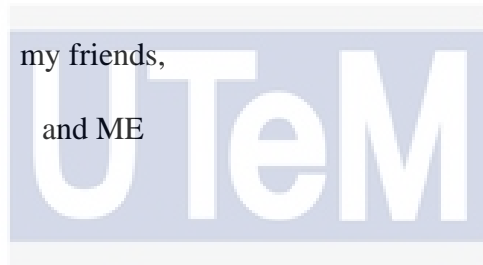
Date : 19 January 2024

اوپنورسیتی بیکنیکل ملیسیا ملاک
UNIVERSITI TEKNIKAL MALAYSIA MELAKA

DEDICATION

To my beloved parents,
my supportive supervisor,
my family,
my girls,
stuffed animals,

my friends,
and ME

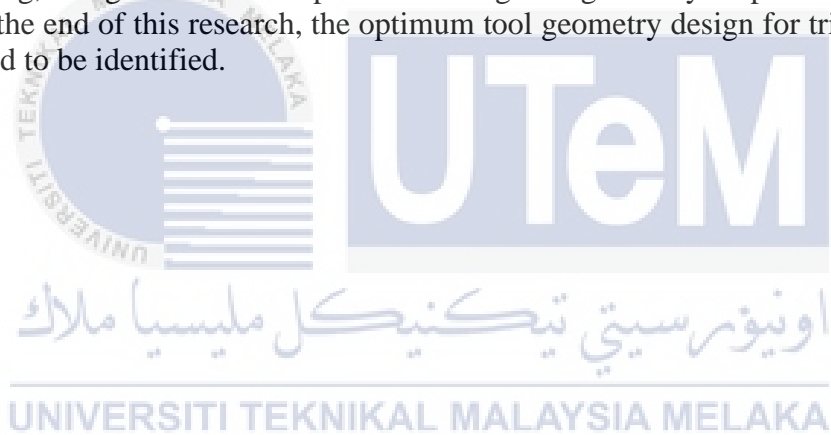


اونيورسيتي تيكنيكل مليسيا ملاك

UNIVERSITI TEKNIKAL MALAYSIA MELAKA

ABSTRACT

Demand of Hybrid Fibre Reinforce Polymer (HFRP) in aerospace industry are increasing due to its properties which are high strength, stiffness, and durability, as well as resistance to corrosion, wear, impact, and fire. Service life of a component is highly relied on the quality of machining. An experimental investigation of the effect of cutting tool design in edge trimming of HFRP was conducted. Edge trimming was used as the machining operation. The focus of the experiment was to identify the optimum tool geometry, namely the number of flutes and helix angle, as well as the impact of it towards surface roughness, cutting temperature, and chip formation during trimming of HFRP. The DoE method was utilized in this research. Taguchi L9 orthogonal arrays were used. The trimming operation was conducted using the router Roland MDX-540. Mitutoyo Surftest SJ-310 was utilized to measure the surface roughness of the machined part. Nikon MM-800 was used to observe the chip formation. The ANOVA approach was used to evaluate all of the collected data. In edge trimming, using the best and optimum cutting tool geometry helped to reduce HFRP damage. In the end of this research, the optimum tool geometry design for trimming HFRP was expected to be identified.



ABSTRAK

Permintaan Hybrid Fiber Reinforce Polymer (HFRP) dalam industri aeroangkasa semakin meningkat disebabkan sifatnya yang mempunyai kekuatan tinggi, kekakuan, dan ketahanan, serta ketahanan terhadap kakisan, haus, hentaman dan kebakaran. Hayat perkhidmatan komponen sangat bergantung pada kualiti pemesinan. Penyiasatan eksperimen tentang kesan reka bentuk alat pemotong dalam pemangkasan tepi HFRP telah dijalankan. Pemangkasan tepi digunakan sebagai operasi pemesinan. Fokus eksperimen adalah untuk mengenal pasti geometri alat yang optimum, iaitu bilangan seruling dan sudut heliks, serta kesannya terhadap kekasaran permukaan, suhu pemotongan, dan pembentukan chip semasa pemangkasan HFRP. Kaedah DoE digunakan dalam penyelidikan ini. Tatasusunan ortogonal Taguchi L9 telah digunakan. Operasi pemangkasan dijalankan menggunakan penghala Roland MDX-540. Mitutoyo Surftest SJ-310 digunakan untuk mengukur kekasaran permukaan bahagian yang dimesin. Nikon MM-800 digunakan untuk memerhatikan pembentukan cip. Pendekatan ANOVA digunakan untuk menilai semua data yang dikumpul. Dalam pemangkasan tepi, menggunakan geometri alat pemotong terbaik dan optimum membantu mengurangkan kerosakan HFRP. Pada akhir penyelidikan ini, reka bentuk geometri alat yang optimum untuk pemangkasan HFRP dijangka dikenal pasti.



ACKNOWLEDGEMENTS

In the Name of Allah, the Most Gracious, the Most Merciful

First and foremost, I want to express my appreciation and praise to Allah, the Almighty, who is both my Creator and my Sustainer, for everything I have experienced since the start of my life. Universiti Teknikal Malaysia Melaka (UTeM), which provided the research platform and authorised the use of equipment in the lab, has my sincere gratitude. I also want to express my gratitude to the Malaysian Ministry of Higher Education (MOHE) for providing the funding.

My sincere gratitude goes out to Ts Dr. Syahrul Azwan Bin Sundi @ Suandi, who is my one and only supervisor, for all of his encouragement, inspiration, enthusiasm, perceptive comments, priceless suggestions, helpful information, practical advice, and never-ending ideas, all of which have been of great assistance to me throughout the course of my research and writing for this thesis. His unwavering kindness and patience in coaching me through the entirety of my Bachelor Degree Project.

Not to forget, from the bottom of my heart I express gratitude to my beloved parents, En. Anuar Bin Ali and Puan Wan Zaharah Binti Wan Chik for their encouragements and who have been the pillar of strength in all my endeavors. Finally, thank you to all the individual(s) who had provided me with the assistance, support and inspiration to embark on my study.

Last but not least, I want to thank myself for not giving up. I know this is not the best, but it is worth my tears, anxiety, and my sleep hours. Been the toughest semester for me, honestly. Finally, I can say, "I SURVIVED".

TABLE OF CONTENTS

	PAGE
DECLARATION	
APPROVAL	
DEDICATION	
ABSTRACT	ii
ABSTRAK	iii
ACKNOWLEDGEMENTS	iv
TABLE OF CONTENTS	v
LIST OF TABLES	vii
LIST OF FIGURES	viii
LIST OF SYMBOLS AND ABBREVIATIONS	xi
LIST OF APPENDICES	xii
CHAPTER 1 INTRODUCTION	13
1.1 Background	13
1.2 Problem Statement	15
1.3 Research Objective	16
1.4 Scope of Research	16
CHAPTER 2 LITERATURE REVIEW	18
2.1 Introduction	18
2.2 Fibre Reinforced Polymer (FRP) material	18
2.2.1 Carbon Fibre Reinforced Polymer (CFRP)	19
2.2.2 Glass Fibre Reinforced Polymer (GFRP)	20
2.2.3 Hybrid Fibre Reinforced Polymer (HFRP)	20
2.3 Machining of HFRP	21
2.3.1 Drilling	21
2.3.2 Milling	21
2.3.3 Edge trimming	22
2.4 Cutting tool in composite machining	22
2.4.1 Polycrystalline Diamond (PCD) type	23
2.4.2 Helical spiral tool type	23
2.4.3 Effect of tool geometry in trimming FRP materials	25
2.5 Machining Parameter	31
2.6 Design of Experiment method (DoE)	32
2.6.1 Taguchi method	32

2.7	Machining performances	33
2.7.1	Surface Quality	33
2.7.2	Machining temperature	37
CHAPTER 3 METHODOLOGY		40
3.1	Introduction	40
3.2	Process flow chart	41
3.3	Experimental setup	41
3.4	Materials details	42
3.5	Tool materials	44
3.6	Specifications of machine	46
3.7	Machining parameters	47
3.8	Jig preparation	47
3.9	Surface roughness	48
3.10	Cutting Temperature	49
3.11	Chip Observation	53
CHAPTER 4 RESULTS		55
4.1	Surface Roughness	55
4.1.1	Down-milling	55
4.1.2	Up-milling	58
4.1.3	Comparison	61
4.2	Cutting temperature	62
4.3	Chip Observation	64
4.4	Optimization using Taguchi Method	65
4.4.1	Signal To Noise Ratio	65
CHAPTER 5 CONCLUSION		72
5.1	Introduction	72
5.2	Conclusion	72
5.3	Recommendation and Future Work	73
APPENDICES		74
References		76

LIST OF TABLES

TABLE	TITLE	PAGE
Table 1:	Summary of effect on tool geometry by previous researchers in trimming of FRP material	29
Table 2:	HFRP stacking direction configuration.	43
Table 3:	Router design details	45
Table 4 :	Taguchi L9 experimental matrix	45
Table 5:	The operating conditions of the machine	46
Table 6	Maximum Cutting Temperature for All Run	51
Table 7	Average surface roughness for transverse direction	57
Table 8	Average surface roughness for longitudinal direction	57
Table 9	Average surface roughness for transverse direction	60
Table 10	Average surface roughness for longitudinal direction	60
Table 11	Response Table for Signal to Noise Ratios	66
Table 12	Response Table for Signal to Noise Ratios	68
Table 13	Response Table for Signal to Noise Ratios	70

LIST OF FIGURES

FIGURE	TITLE	PAGE
Figure 1.1	Trends in the use of composite material in Airbus aircraft. (Xu, Y 2018)	13
Figure 2.1	Usage of composite materials in aerospace structures: (a) Boeing 787 and (b) Airbus A380 (Abramovich, 2017)	19
Figure 2.2	Comparison between End Milling and Edge Trimming (Sheikh-Ahmad, 2009)	22
Figure 2.3:	End Mill geometry (courtesy of Sandvik Coromant)	24
Figure 2.4:	Burr tool (courtesy of Fullerton)	24
Figure 2.5:	PCD and CVD-diamond coated tools used (Iker Urresti, 2022)	25
Figure 2.6:	Tungsten carbide tool (Deviprakash Jyothi Devan, 2022)	26
Figure 2.7:	Routers utilised in the experiment (Chunliang Kuo, 2021)	27
Figure 2.8:	three different geometrical features of router (S. A. Sundi, 2021)	27
Figure 2.9:	Two different cutting tool design: Left-Right Edge Milling (top), Right Edge Milling Tool (bottom) (Fu-Ji Wang, 2020)	28
Figure 2.10:	Details of investigated cutting tools (T1, T2 and T3) (Rangasamy Prakash, 2016)	29
Figure 2.11:	Arithmetic mean roughness value Ra (https://roguepiercing.co.uk/2019/08/23/high-quality-part-4-surface-finish/)	34
Figure 2.12:	Comparison of surface roughness for different machining conditions; (a) 3000 rpm; (b) 6000 rpm; (c) 9000 rpm (Rangasamy Prakash, 2016)	35

Figure 2.13: (a) measuring position, (b) result of line arithmetic average roughness Ra (Fu-Ji Wang, 2020)	36
Figure 2.14 : Fracture patterns in carbon fibres created by cutting tools in SEM images (Chunliang Kuo, 2021)	37
Figure 2.15 Experimental setup (Guoyi Hou, 2021)	38
Figure 2.16 Cryogenic conditions (left), dry conditions (right) (Dhiraj Kumar, 2020)	39
Figure 3.1: Flow of the overall research	41
Figure 3.2 Overall Experimental setup	42
Figure 3.3: The HFRP panel were cut into smaller pieces for the experiment.	44
Figure 3.4: Router tools	45
Figure 3.5: Roland MDX-540.	46
Figure 3.6: Details of the jig	47
Figure 3.7: Jig to hold the specimens.	48
Figure 3.8 HFRP Panel	48
Figure 3.9: SJ-310 for measuring surface roughness.	49
Figure 3.10 Cutting Temperature Recordings	49
Figure 3.11 Opening the Recording from Existing File.	50
Figure 3.12 Step to analysed cutting temperature.	50
Figure 3.13 Fluke SmartView setting.	51
Figure 3.14 Nikon MM-800	54
Figure 4.1 Average Surface Roughness for transverse direction	56
Figure 4.2 Average Surface Roughness for longitudinal direction	56
Figure 4.3 Average Surface Roughness for transverse direction	59
Figure 4.4 Average Surface Roughness for Longitudinal direction	59

Figure 4.5 Comparison of Average Surface Roughness for transverse direction for down milling and up milling	61
Figure 4.6 Comparison of Average Surface Roughness for longitudinal direction for down milling and up milling	62
Figure 4.7 Lowest Cutting Temperature	63
Figure 4.8 Highest Cutting Temperature	64
Figure 4.9 Bar Chart of Maximum temperature vs Cutting Tool	64
Figure 4.10 Chip formation	65
Figure 4.11 Mean of SN ratio for smaller the better characteristics of surface roughness up-milling.	67
Figure 4.12 Normal Plot of Residuals	67
Figure 4.13 Mean of SN ratio for smaller the better characteristics of surface roughness down-milling.	69
Figure 4.14 Normal Plot of Residuals	69
Figure 4.15 Mean of SN ratio for smaller the better characteristics of Temperature.	71
Figure 4.16 Normal Plot of Residuals	71

LIST OF SYMBOLS AND ABBREVIATIONS

D, d	-	Diameter
FRP	-	Fibre Reinforce Polymer
CFRP	-	Carbon Fibre Reinforce Polymer
GFRP	-	Glass Fibre Reinforce Polymer
HFRP	-	Hybrid Fibre Reinforce Polymer
a_e	-	Axial depth of cut
a_p	-	Tool diameter step over
Ra	-	Arithmetic Mean Roughness Value
V_c	-	Cutting Speed
V_f	-	Table feed
f_z	-	Feed per tooth



LIST OF APPENDICES

APPENDIX	TITLE	PAGE
Appendix A	Gantt chart PSM 1	74
Appendix B	Gantt chart PSM 2	75



CHAPTER 1

INTRODUCTION

1.1 Background

These days, composite materials are gaining attention from numerous industries due to their benefits and unique mechanical properties that cannot be found in any metallic materials. The term "composite" can be defined as a material that is made with a combination of two or more materials that have different properties to achieve desirable mechanical properties. Fibre-Reinforced Plastic (FRP) is one of the composite materials that have attracted substantial interest from the aerospace industry, especially due to their greater specific strength and modulus, light weight, adjustable deformation behaviour, and high corrosion resistance (Saptarshi Maiti, 2022) Figure 1.1 shows the increasing trend of the usage of composite material in Airbus aircraft.

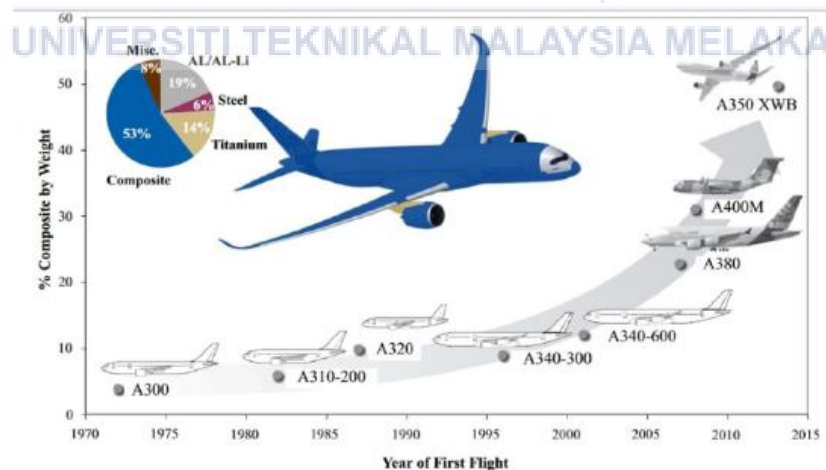


Figure 1.1 Trends in the use of composite material in Airbus aircraft. (Yingjie Xu, 2018)

Two main FRP materials used in aero-structural components are Glass Fibre Reinforced Polymers (GFRP) and Carbon Fibre Reinforced Polymers (CFRP). Although the aerospace industry has been using CFRP for a variety of components, including aircraft fuselages, wings, and tail sections, to lighten the load and improve fuel efficiency, it can be expensive. So, the industry slowly changed the CFRP to a new FRP known as Hybrid Fibre Reinforced Polymer (HFRP) after its introduction because it has high strength, stiffness, and durability, as well as resistance to corrosion, wear, impact, and fire. HFRP is a more cost-effective material compared to CFRP because it offers similar benefits at a lower price. It may however note that most of studies were aimed at milling/trimming for CFRP and a rigorous study for milling/trimming of HFRP has not been attempted to. Hence, this chapter will only discuss milling/trimming related to the HFRP material as the focus material.

Generally, machining composite materials is very different from machining metallic materials. It could be difficult to machine composite materials compared to metallic materials, even though theoretically and technologically they are the same. Milling or trimming is one of the necessary machining operations that is typically used as a post- or finishing operation to obtain the requisite dimensioning accuracy (S. A. Sundi, 2021). When trimming composite materials, it is important to consider the unique properties of composites, such as their anisotropic nature and directional properties, as they will create problems in machining such as rapid tool wear, fibre delamination, high cutting force, fibre pull-out, and fibre-matrix debonding.

In order to minimise damage to the machined surface and extend tool life, it is essential to choose the right machining settings, tool geometry, and materials when working with HFRP. However, HFRP is a heat sensitive material where it can easily warp or deform when it is trimmed. Therefore, this study focuses mainly on tool geometry, where machining of HFRP

demands special tools and methods after taking the high strength of HFRP into consideration. Thus, the purpose of this study is to determine the effects of cutting tool geometry on the milling and trimming of HFRP.

The objective of this study is to identify the most optimum cutting tool geometry for milling or trimming HFRP, as measured by the number of flutes and the helix angle. As studies relating to the machining of HFRP have been relatively scanty and there are limited studies were found focusing on milling or trimming of HFRP, therefore this research is initiated. Machinability in trimming of HFRP shall be evaluated namely the surface quality, cutting temperature and the chip formation.

1.2 Problem Statement

There were few problems that need immediate solutions when it comes to milling/ trimming of composite material especially HFRP material. This is due to various material properties namely metal as well as fibres/epoxy have been laminated in one single composite panel.

Due to their inhomogeneous structure, high hardness, and abrasive character of the reinforcing phase, composites continue to be challenging to process, which poses a difficulty for the industry. (J. Sheikh-Ahmad, 2012)

In addition, there were numerous issues arise during the milling of fibre-reinforced composite (FRP) materials, including delamination damage factor or surface damage, surface roughness, fibre pull out and matrix failure associated with it due to material characteristics, specified machining cutting parameters, tool material and geometry, and fibre orientation. (Priyansh Patel, 2018)

Last but not least, it would be a costly loss to the industry could result from any machining flaws that appear on the milling surface. Unfortunately, the low machinability of FRP composites frequently results in major flaws like delamination, which ultimately raises maintenance costs. (M C H Ling 2020)

1.3 Research Objective

The objectives of this research are stated as below:

- a) To determine the effect of the tool geometrical feature namely the number of flutes and the helix angle on the surface roughness and temperature during trimming of HFRP material.
- b) To observe the impact of the chip formation when various combinations of tool geometry are deployed in trimming of HFRP material.
- c) To identify the optimum cutting tool geometry for trimming a specific HFRP material.

1.4 Scope of Research

For this research, an actual aerospace component Hybrid Fibre Reinforced Polymers (HFRP) was used to validate the tool geometry. Tool geometry features that were studied were the number of flute and helix angle for both left and right. Uncoated solid carbide router tools were selected as the tool material. This experiment ran under constant cutting parameters

with cutting speed, (V_f) of 150m/min and spindle speed, (N) of 7518 rpm using Router Roland MDX-540 machine. Down cut and up cut was the mode of machining direction to be applied. Axial depth of cut (a_e) to the HFRP specimens' thickness and a complete 100% of the tool diameter step over (a_p) were applied for the edge trimming operation. Mitutoyo SJ-310 was utilized to determine the surface roughness Ra of the trimmed surface. Longitudinal and transverse were considered during measurement of the surface roughness. For further observation of the chip, Nikon MM-800 was used. All the gathered data shall be analysed via ANOVA analysis.



CHAPTER 2

LITERATURE REVIEW

2.1 Introduction

In this chapter, a few literature studies were taken forward to give a better understanding of the research work.

2.2 Fibre Reinforced Polymer (FRP) material

Fibre Reinforced Polymer composite (FRP) has garnered the most attention out of all composite materials due to its many benefits, including its high strength to weight ratio, light weight, good impact resistance, sound mechanical qualities, and lower price when compared to metal products. In FRP, the reinforcement material can be either natural or synthetic fibres, or a combination of both, while the matrix is formed of polymer (Priyansh Patel, 2018). FRP composites have been used commercially as the primary design structures for several well-known goods, including the Ford GT40 racing car body, the Boeing 787, 767, and 777 landing gears, and marine equipment (such as petrol boats). (Eshetu D. Eneyew, 2014)

In recent years, several studies have focused on the machining of FRP composite materials due to increasing demand in the aerospace industry. A significant portion of contemporary aircraft structures, such those of the Boeing 787 or Airbus A380 (see Figure 2.1), are made of carbon, glass, and aramid fibres. (Abramovich, 2017)

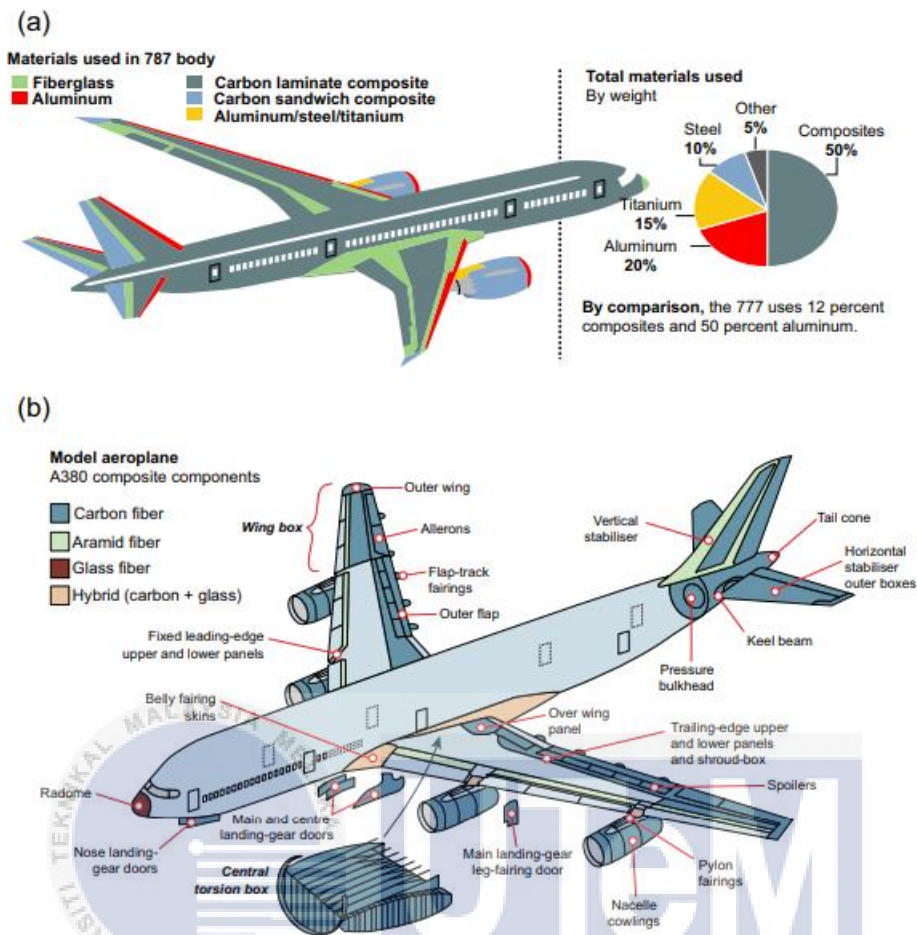


Figure 2.1 Usage of composite materials in aerospace structures: (a) Boeing 787 and (b) Airbus A380 (Abramovich, 2017)

2.2.1 Carbon Fibre Reinforced Polymer (CFRP)

The term "CFRP" refers to a composite material comprised of carbon fibres embedded in a polymer matrix. It is a synthetic fibre formed from carbonaceous materials, either naturally occurring (because carbon has poor performance, it is not utilised in structures needing strain) or synthetically produced from polyacrylonitrile (high yield on carbon), known as "PAN" (from Polymer acrylic nitrile) (Marcelo André Santiago Barros, 2015). In the aerospace industry, Carbon Fibre Reinforced Polymer (CFRP) composites are frequently employed due to their exceptional lightweight material features, tensile strength, and stiffness capabilities. (Deviprakash Jyothi Devan, 2022). Due to the presence of two phases

of materials in CFRP composites with significantly different mechanical and thermal properties, there are complicated interactions during machining between the matrix and the reinforcement. (Rangasamy Prakash, 2016).

2.2.2 Glass Fibre Reinforced Polymer (GFRP)

Glass fibres embedded in a polymer matrix make up the composite material known as GFRP, or Glass Fibre Reinforced Polymer. Since the 1960s, silicon dioxide (SiO_2) has been a common raw material in the aircraft industry. SiO_2 and other oxides primarily separate "E-glass" and "S-glass" with differing elastic moduli and specific strengths. Because "E" fibres are more frequently employed in aircraft structures than "S" fibres and have greater resistance to electrical conductivity, they are also referred to as "electric" fibres. (Marcelo André Santiago Barros, 2015)

2.2.3 Hybrid Fibre Reinforced Polymer (HFRP)

The advanced Fibre Reinforced Polymer (FRP) composite known as hybrid uses two or more different types of fibre reinforcement in a polymer matrix. (Mohd Azuwan Maoinser, 2014). Since 1970, Hybrid Fibre Reinforced Polymer (HFRP) composites have been used to tune the unique properties of fibre-reinforced polymer (FRP) composites. These composites combine the benefits of both fibres while concurrently minimising their disadvantages. Major composite manufacturers have been drawn to creating HFRP composites because to the high strength carbon fibre and high elongation glass fibre in polymers. (Tan, 2015)

2.3 Machining of HFRP

The process of machining entails using a machine tool to remove, shape, or cut material from a workpiece. It is a form of subtractive manufacturing that makes use of machine tools to remove undesirable material from a bigger piece of material in order to mould the material into the desired shape. There are several materials that can be machined, including metal, wood, plastic, ceramic, and composite materials. There is few machining processes of HFRP which are drilling, milling and trimming.

2.3.1 Drilling

In the machining process of drilling, round holes are made in a workpiece using a drill bit, which is a rotary cutting tool. As it drills, the drill bit is rotated quickly while being forced against the workpiece to remove any chips or swarf. A rotating cutting tool is used in the CNC drilling process to create round holes in a stationary workpiece. An area of research that has received a lot of attention is drilling-related damage and ways to optimize the damage.

2.3.2 Milling

A workpiece is cut using cutting tools that are rotated at certain speeds during the milling process. The workpiece is held in place by using a fixture. Then the cutting begin to remove material when it touches the workpiece. Simply said, milling is the act of removing material by feeding a workpiece past a rotating cutter with several teeth. Milling of FRP composite is the most crucial and widely used method in industry for removing extra material, producing high-quality surfaces, and joining composite material structure. (Priyansh Patel, 2018)

2.3.3 Edge trimming

Edge trimming is a cutting technique that is frequently used in the production of composite material parts to get rid of extra material after demoulding. To bring Fibre Reinforced Polymer (FRP) composites to the desired final dimensions, finish edge trimming is frequently necessary. Edge trimming may cause damage to the material, though, which can lower the failure stress of carbon fibre polymer composites because of the inhomogeneous nature of FRP composites. Because edge trimming is a crucial step in creating aero-structural components, these issues could be problematic for the aerospace manufacturing industry.

Figure 2.2 shows the comparison between milling and edge trimming.

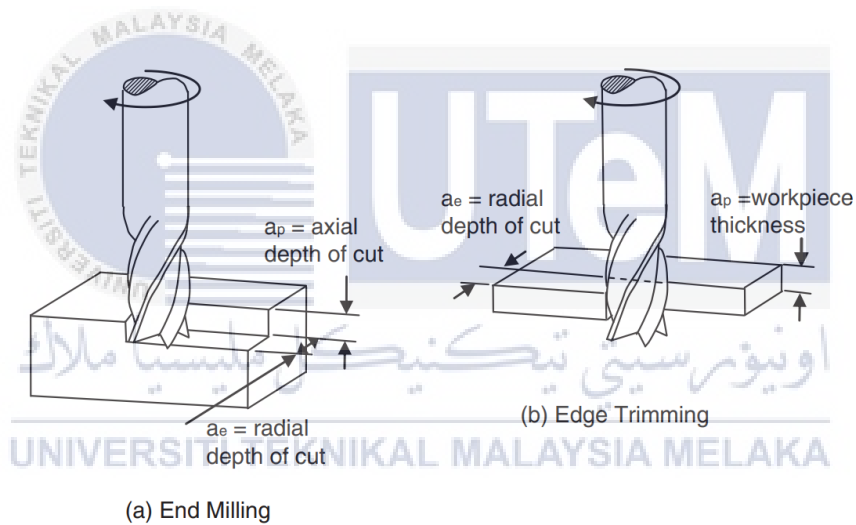


Figure 2.2 Comparison between End Milling and Edge Trimming (Sheikh-Ahmad, 2009)

2.4 Cutting tool in composite machining

Selection of tool material and tool geometry are the most crucial because it will affect the surface quality of the final goods. Hence why, for the purpose of machining FRPs, a range of cutting tool materials and geometries are available. The diverse features of FRP products resulting from the various shapes, types of reinforcement, matrices, and volume fraction of reinforcement fibres that are used for various applications are one cause for this variability

in tools. (Rangasamy Prakash, 2016). Generally, there are 2 common types of cutting tool for composite namely polycrystalline diamond (PCD) and helical spiral.

2.4.1 Polycrystalline Diamond (PCD) type

Polycrystalline Diamond (PCD) cutting tools are widely used in various industries due to their excellent mechanical properties. PCD tool mainly made of two primary components from carbide material which are insert and body. Due to the technology and manufacturing procedures necessary to make the tool, such as the high pressure and temperature required for the sintering process causing the tool to be more expensive compared to normal solid carbide tools. (S. A. Sundi, 2021). Although the PCD cutting tools are pricier compared to carbide tools, but it can reduce manufacturing costs for massive production due to longer tool life and the results are more consistent. PCD cutting tool are ideal for cutting abrasive materials such as Carbon fibre or fibreglass, which can easily wear out carbide tools.

2.4.2 Helical spiral tool type

Cutting tools that use helical paths to remove material from a workpiece are known as helical spiral tools. The tool's helix produces a spiral cutting effect that significantly lowers tool pressure and improves form accuracy by reducing deflection. a situation like cutting materials if no considerations are required, helical spiral tools are the best choice since their helical cutting edge minimises material contact during the cut. To accommodate the majority of milling applications, helical spiral tools come in a variety of sizes, shapes, and helix angles. They can be used for roughing, semi-finishing, or finishing to speed up the machining process. End mill and burr tool are common type of helical spiral tool.

End mill (figure 2.3) known in cutting metallic materials. End mills are available in a wide range of lengths, diameters, flute number, and type. They are selected based on the material they will be cutting, and the level of surface quality needed for the project.



Figure 2.3: End Mill geometry (courtesy of Sandvik Coromant)

Burr tool (figure 2.4) also referred as multi-tooth, knurled, and diamond interlocking by researchers around the world. This type of tool was commonly design with right and left helix shape with certain angles. Due its effectiveness in trimming FRP materials, more studies on the tool geometry features were done by researchers worldwide in order to get the most optimum quality outcomes.



Figure 2.4: Burr tool (courtesy of Fullerton)

In this work focusing on burr tool type with different tool geometry design known as number of flute and helix angle.

2.4.3 Effect of tool geometry in trimming FRP materials

In the recent present work focusing on the optimization of tool geometry features in machining FRP materials especially on trimming operation. Iker Urresti et al. (2022), were one of the recent researchers who performed an experimental study of surface integrity during CFRP trimming using different tool geometry known as PCD and diamond CVD-coated carbide mills with some variations on number of tooth and helix angle for both mentioned tool (figure 2.5). Authors conclude that the presence of helix and axial rake angles makes it possible to machine CFRP and produce a good surface quality with greater flank wear values and somewhat extending tool life.

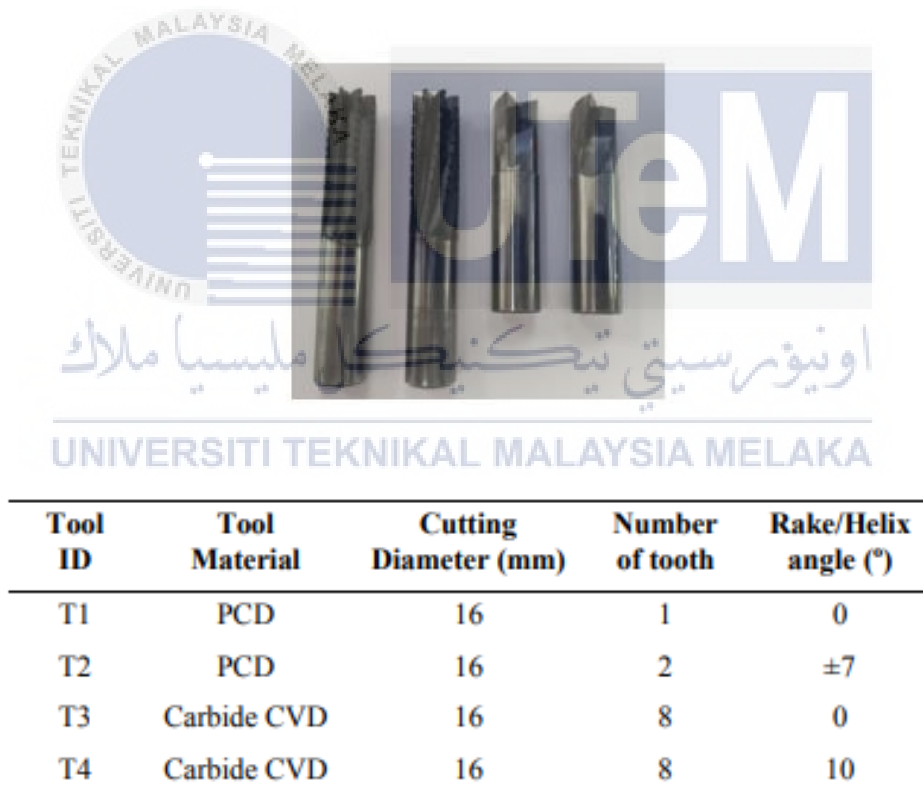


Figure 2.5: PCD and CVD-diamond coated tools used (Iker Urresti, 2022)

Deviprakash Jyothi Devan et al. (2022), studied on tool wear in edge trimming of CFRP using tungsten carbide cutters (figure 2.6). They confirmed that the cutting parameters (feed speed, cutting speed, and depth of cut) and the response variables (surface roughness,

temperature, force, and power) were clearly correlated through experimental tests and additional simulations. A tool life equation for tungsten carbide tools was created as a result of this relationship, which took cutting speed, feed speed, and depth of cut into account. Lower cutting speed, feed speed, and depth of cut settings were found to extend the tool's life.



Figure 2.6: Tungsten carbide tool (Deviprakash Jyothi Devan, 2022)

An investigation by Chunliang Kuo et al. (2021), considered three types of different geometries CVD-coated tungsten carbide tools namely straight flute, nicked helical flute and cross flute (figure 2.7). The authors discovered that the helical flute and cross flute geometric arrangement enables the secondary cutting edges to counteract the primary cutting edges' cutting forces, dispersing the forces and reducing tool wear. High cutting forces and significant flank wear were created by the straight flute geometry, whereas low cutting forces and minimal flank wear were produced by the helical flute geometry. Despite the effects of chattering, straight-flute routers created surfaces with smooth surface textures on the topographies of machined surfaces. Numerous transverse strands were taken out of the nicked helical-flute routers, demonstrating a connection between oblique cutting and the direction of the woven fibres. The cross-flute router provided continuous shearing motions, smeared the surface, and permitted the localised adherence of chips and swarf due to its circular array of symmetric primary and secondary cutting edges.

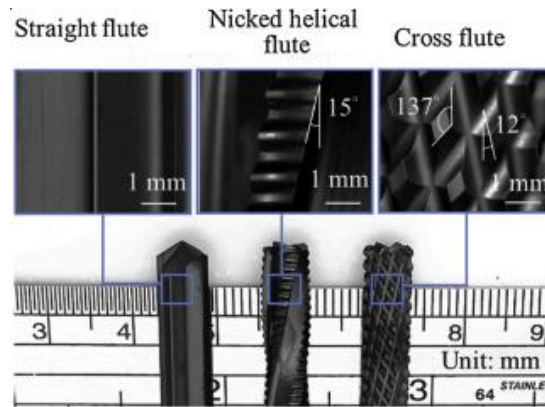


Figure 2.7: Routers utilised in the experiment (Chunliang Kuo, 2021)

Meanwhile, Sundi et al. (2020), performed a series of a comparative study on a few different micro-grain of router tools which categorized into fine (T1), medium (T2), and smooth (T3) type (figure 2.8) in trimming of CFRP material. Authors discovered that fine tool (T1) produced the highest surface roughness value (Ra), while smooth tool (T3) produced the lowest surface roughness in relation to the total averaged Ra value.



Figure 2.8: three different geometrical features of router (S. A. Sundi, 2021)

In a different study, Fuji wang et al. (2020) proved that his new tool, known as the left-right end mill tool (Figure 2.9), effectively minimizes the damages on machined surfaces, especially those related to delamination, compared to the standard helical helix tool with a 30° helix angle for small cutting depths.

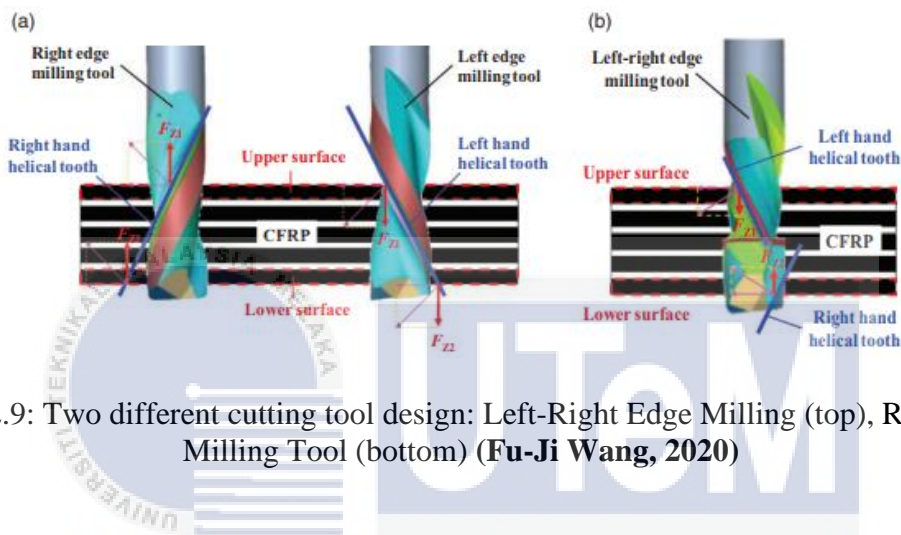
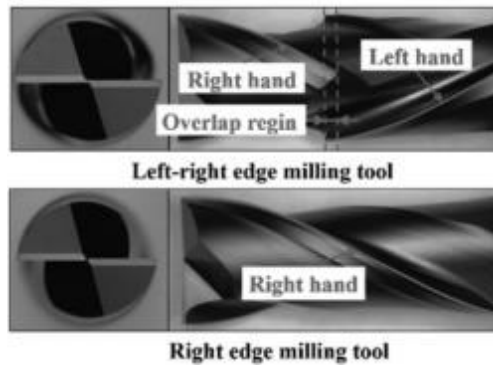
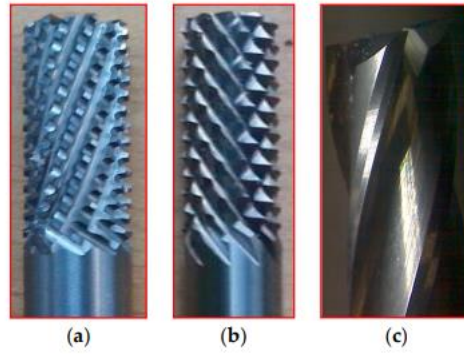


Figure 2.9: Two different cutting tool design: Left-Right Edge Milling (top), Right Edge Milling Tool (bottom) (Fu-Ji Wang, 2020)

Earlier before, Prakash et al. (2016) have performed an experimental investigation on the effect of the trimmed surface quality in high-speed milling of CFRP composites by modifying three distinct types of tool geometries, which were divided into two different detailed router type tool (T1 and T2) and helical helix geometry (T3) (figure 2.10). They discovered that the router tool with the trapezoidal tooth (T1), which produced a smaller cutting force and a satisfactory surface roughness (Ra) with no delamination, was the best of the three tools. Meanwhile, the other router tool with pyramidal tooth (T2) produced a greater cutting force and surface roughness (Ra) compared to the first tool. When compared to tools T1 and T2, tool helical helix end mill T3 produced more delamination and a higher cutting force.



Tool	Specification	Image of the Tool	Tooth Shape	Tooth Profile
Tool T1	Pitch = 3.42 mm			
	No. of flutes—12			
	Tooth Shape—Trapezoidal			
Tool T2	Pitch = 2.42 mm			
	No. of flutes—12			
	Tooth Shape—Pyramidal			
Tool T3	Helix angle 30°			
	No. of flutes—4			
	Tooth Shape—Helical fluted			

Figure 2.10: Details of investigated cutting tools (T1, T2 and T3) (Rangasamy Prakash, 2016)

Table 1: Summary of effect on tool geometry by previous researchers in trimming of FRP material

No	Researchers	Year	Tool type/ geometry	Findings
1	Prakash et al.	2016	router type tool (T1 and T2) and helical helix end mill (T3)	The best of the three tools was the router with the trapezoidal tooth (T1), which provided a lower cutting force and a reasonable surface roughness (Ra) without delamination. the pyramidal-toothed router tool (T2) produced more cutting force

				and surface roughness (Ra) than the first tool. Helical helix end mill (T3) exhibited the highest cutting force among those three tools.
3	Wang et al.	2020	Two different cutting tool design: left-right edge milling, right edge milling tool with 30° helix angle	Newly tool (left-right edge milling) effective to remove burrs and reached the satisfactory in surface quality.
4	S. A. Sundi et al.	2020	Three different micro-grain of router tools which categorized into fine (T1), medium (T2), and smooth (T3)	Smooth tool (T3) the minimized surface roughness value (Ra). Fine tool (T1) the highest surface roughness value (Ra). Medium tool (T2) in between T1 and T2 for surface roughness value (Ra).
5	C. Kuo et al.	2021	straight flute, nicked helical flute and cross flute	Straight flute produced greater cutting forces and severe flank wear. In other hand it produced smooth surface texture. Helical flute produced low cutting force and flank wear. Nicked helical router drew out a lot of transverse fibre.
6	D. J. Devan et al.	2022	tungsten carbide tool	A clear relationship between cutting parameters and response variables that led to the enhancement of a tool life equation for tungsten carbide tools were established.
7	Iker Urresti et al.	2022	PCD and CVD-diamond coated tools	For composite machining, low helix and axial rake angles are

				advised to reduce the axial cutting force component and prevent top and bottom layer delamination.
--	--	--	--	--

2.5 Machining Parameter

In machining operations, cutting tools and machining parameters are closely related. The performance of the machining process is directly impacted by the choice of the cutting tool and machining settings. Some of the relevant machining parameters for conventional machining include the following:

Cutting speed or cutting velocity:

$$\text{Cutting speed (m/min)} = \frac{\pi \times D \times n}{1000}$$

Where:

D: tool diameter

n: spindle speed (RPM)

Feed per tooth:

$$f_z = \frac{V_f}{n \times Z_c}$$

Where:

V_f : Feed (mm/min)

Z: Number of Flute

Feed rate and cutting speed have a complicated and interdependent relationship with tool geometry. Spindle speed, the number of flutes or teeth on the cutting tool, and chip load all influence feed rate and cutting speed. To achieve efficient and effective material removal, a smooth finish, and lower manufacturing costs, the feed rate and cutting speed must be optimised. Same goes with tool geometry, it must be optimised in order to get the desired machining results.

2.6 Design of Experiment method (DoE)

The analysis of the relationship between the response and the variables is the main goal of the Design of Experiment. Experimental data are needed to study the relationship between the response and self-governing variables (T. D. Jagannatha, 2019). It is a methodical strategy for gathering information and discovering new things.

2.6.1 Taguchi method

The Taguchi method is a process/product optimisation technique based on eight steps of planning, carrying out, and assessing the outcomes of matrix experiments to enhance the desired properties and decrease the number of flaws by analysing the major process variables and optimising the procedures or design to produce the best outcomes. C. L. Tan (2015) applied the Taguchi L_{27} orthogonal array experimental design to optimize the machining parameters during drilling of HFRP material to improve the surface quality and reduce delamination.

In 2014, Maoinsere et al. have studied the effect of machining parameters on drilling thrust force for HFRP composite. He discovered the optimum way of drilling HFRP composite through thrust force minimization with the aid of analysis of variance (ANOVA) and signal to noise (S/N) ratio analysis. Based on his study, The optimal drilling conditions are a low feed rate of 0.02 mm/rev, a tiny drill point angle of 85°, and a medium cutting speed of 106 m/min. In accordance with the confirmation experiment, which yielded a drilling thrust of 6.92 N, this optimisation method has provided a value of 6.4 N, and this value is within 91.89% confidence. However, the production rate can be enhanced by employing a greater cutting speed that leads to a higher feed speed because this factor has a less substantial impact on the thrust force value than the feed rate and drill point angle.

2.7 Machining performances

The cutting performance and machining quality of the tools used in composite machining vary depending on the cutting circumstances. Cutting conditions, tool life, and surface quality of the machined parts are all heavily influenced by the tool material, tool geometry, and cutting conditions (Deviprakash Jyothi Devan, 2022)

2.7.1 Surface Quality

Previous studies have primarily concentrated on surface roughness as one of the important outcomes as precision surface roughness measurements are needed in the aerospace sector to guarantee the dependability and safety of aircraft parts. The relative smoothness of a surface's profile is gauged by its surface roughness. Surface roughness can be measured using a variety of techniques, such as geometric analysis and scanning probe microscopy. There are few surface roughness measurements such as roughness average (Ra), root mean square (RMS), and average maximum height (Rz).

In this research R_a will be used as the surface roughness measurement. It is the typical parameter used for surface roughness. It is the arithmetic average of the measured surface heights distributed over a surface as in figure 2.11. However, R_a is less sensitive to significant peaks and valleys and gives a general description of height differences on the surface.

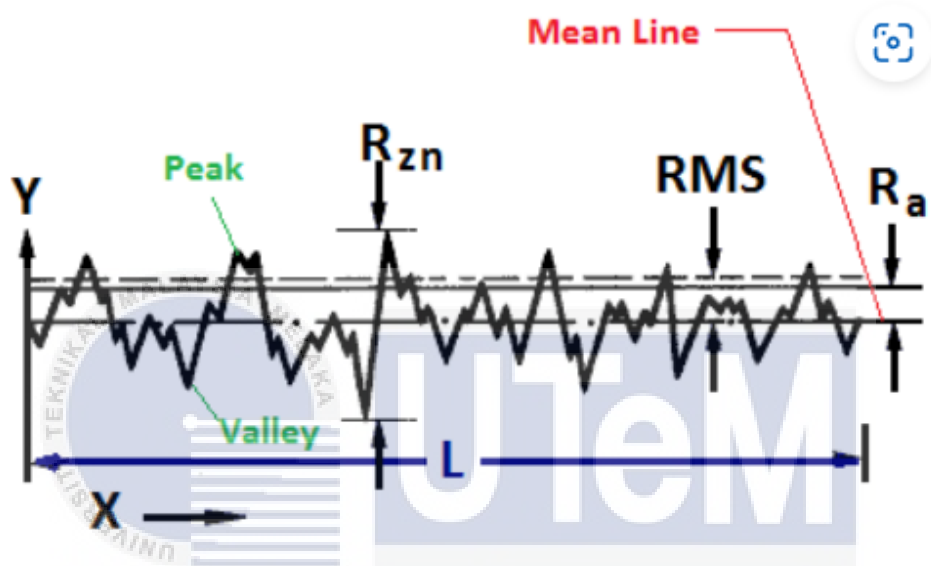


Figure 2.11: Arithmetic mean roughness value R_a
[\(https://roguepiercing.co.uk/2019/08/23/high-quality-part-4-surface-finish/\)](https://roguepiercing.co.uk/2019/08/23/high-quality-part-4-surface-finish/)

UNIVERSITI TEKNIKAL MALAYSIA MELAKA

A comparison study of router tools and end mill tool by (Rangasamy Prakash, 2016) discovered that router tools with trapezoidal shape tooth T1 gives the acceptable surface roughness value compared to T2 and T3. Pyramidal shape tooth T2 give the highest surface roughness value due to the existence of a sharp cutting edge. Meanwhile the surface roughness for end mill T3 were less at all spindle speed due to the scooping action of the helical flutes during machining. Figure 2.12 represents the comparison of surface roughness for 3000 rpm, 6000 rpm, and 9000 rpm.

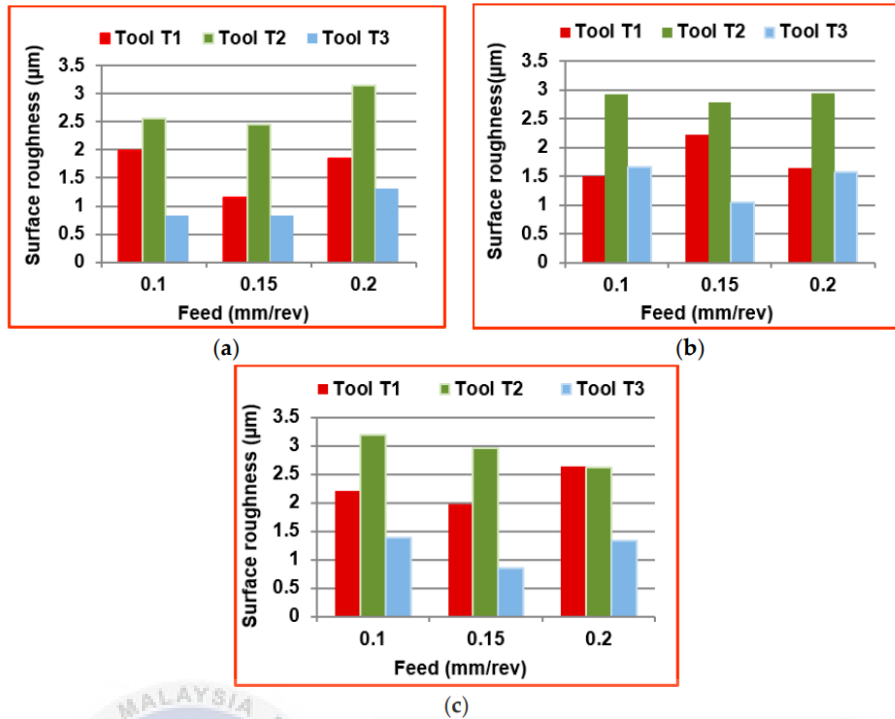


Figure 2.12: Comparison of surface roughness for different machining conditions; (a) 3000 rpm; (b) 6000 rpm; (c) 9000 rpm (**Rangasamy Prakash, 2016**)

In a study by Fuji wang, 2020 of surface damage reduction of dry milling with using new tool known left-right edge milling tool on CFRP. Authors discovered that the surface roughness value (Ra) for the left-right edge milling tool was larger than using the right edge milling. They also discovered that the (Ra) is directly proportional to the feed per tooth for both tools. Figure 2.13 shows the line roughness Ra curve.

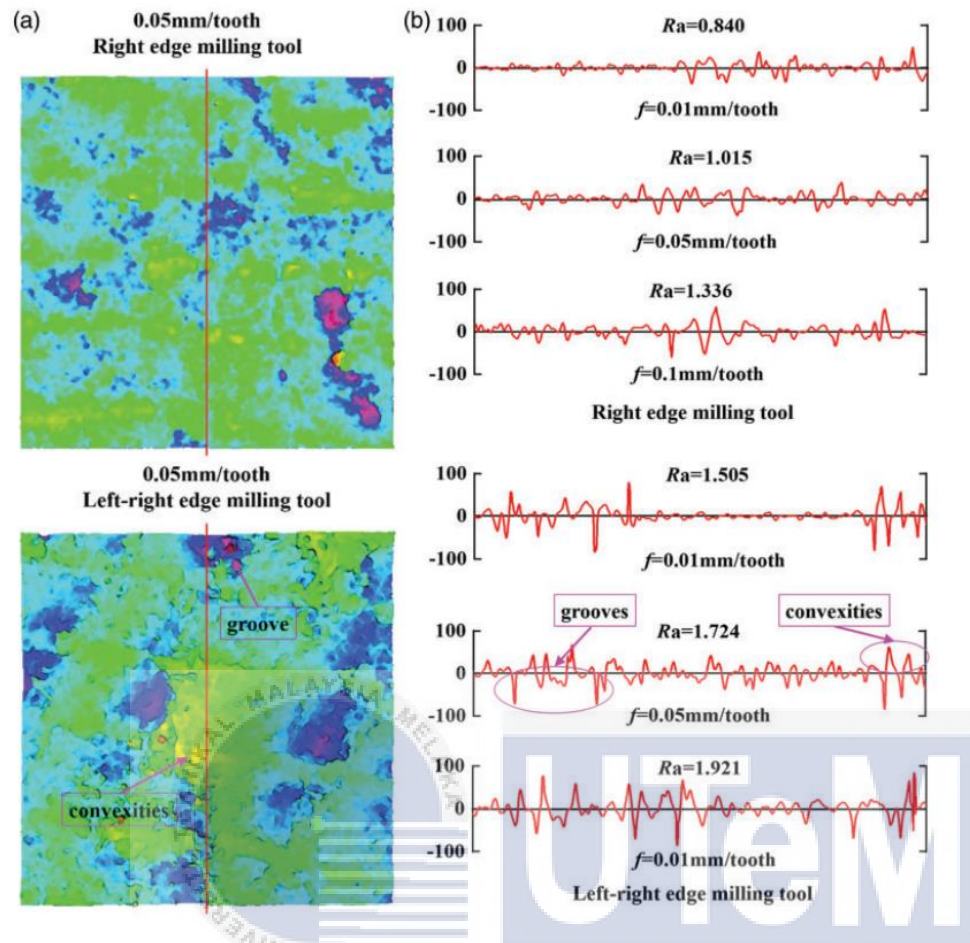


Figure 2.13: (a) measuring position, (b) result of line arithmetic average roughness Ra (Fu-Ji Wang, 2020)

C. Kuo et al. (2021), discovered that Straight-flute routers led to tensile fracture of the fibres that were bent in the right direction. Helix-flute routers, however, led to shearing and bending fractures. Finally, cross-flute routers contributed to the intermittent buckling or crushing of fibres. Figure 2.14 shows the fractured pattern of carbon fibre using SEM. The authors also proved that surface quality was heavily influenced by cutting tool geometrical design. With the presence of a sharp cutting edge of pyramid shaped tooth profile of T1, causing it having a higher surface roughness (Ra) value compared to trapezoidal tooth (T1) and helical flute (T3).

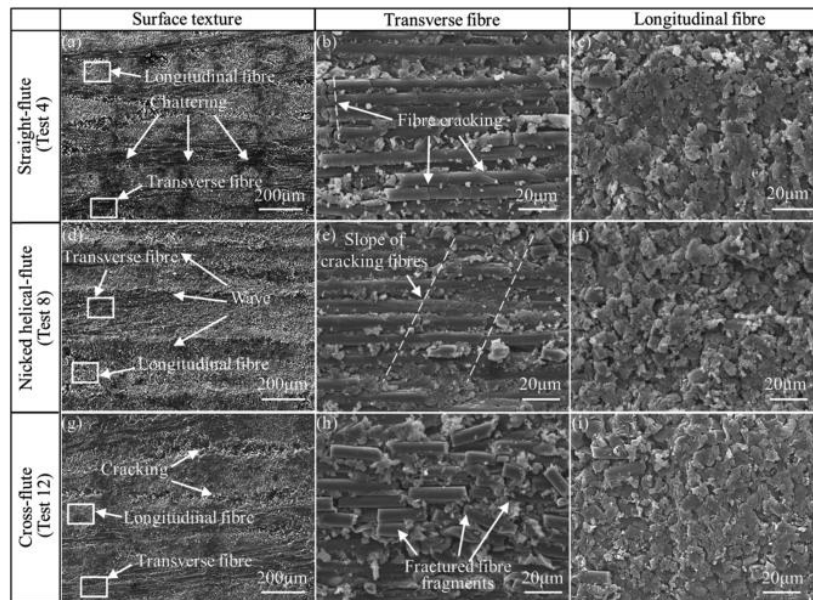


Figure 2.14 : Fracture patterns in carbon fibres created by cutting tools in SEM images (Chunliang Kuo, 2021)

In more recent work by (Deviprakash Jyothi Devan, 2022) reported that surface roughness (Ra) parameters are inversely proportional to cutting speed. Ra can be decreased through a reduction in chip per tooth, less matrix and fibre deformation, and an increase in cutting speed. In other hand, surface roughness parameters are directly proportional to feed speed and depth of cut. An increase in feed speed can result in increased heat generation, higher chip thickness, and chatter, which can prevent the workpiece from being completely machined, higher roughness.

2.7.2 Machining temperature

A crucial consideration when working with composite materials in aircraft components is machining temperature. Due to their heat sensitivity, composite materials can have their microstructure changed by machining temperatures, which may leave residual stress that shortens the component's fatigue life. Several variables, including cutting speed, feed rate and tool geometry, can have an impact on the cutting temperature, which is the average

temperature of all points of contact between the cutting tool and the workpiece. (Petr Masek, 2021)

In 2021, a study by G. Hou et al. in his study about the impact of high temperature on the CFRP cutting mechanism, found that a high temperature that below transition glass temperature (T_g) of matrix obviously affects the development of chips and subsurface damage as the resin will become softer and lose some of its strength, which lead to severe fibre-matrix debonding and matrix cracking. Moreover, for temperature that above T_g would cause the resin matrix to transform into molten state and nearly entirely lose its ability to sustain the machined fibres. The flank face and cutting lip would cut off the molten state matrix causing typical thermal subsurface damage.

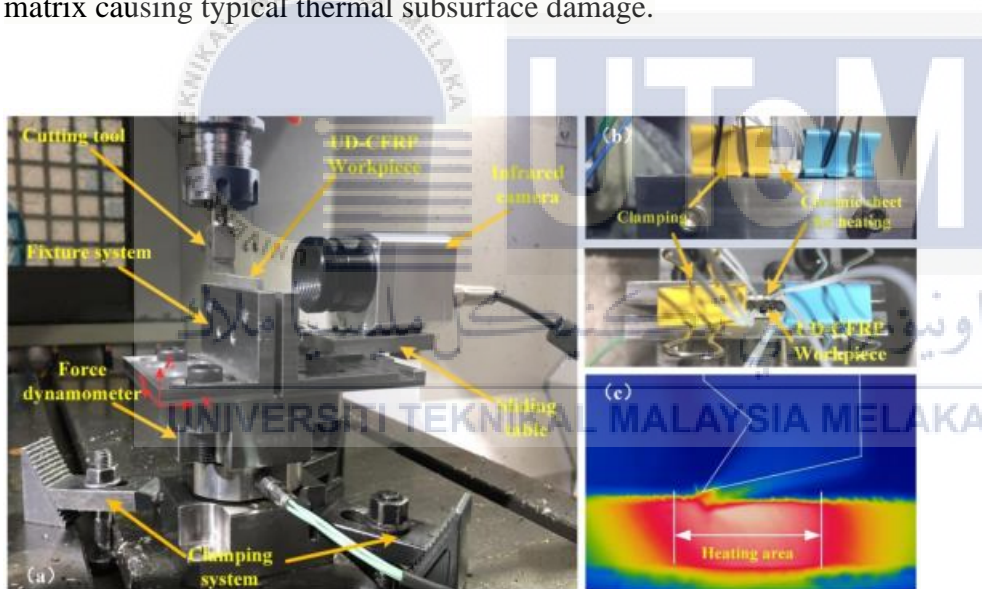


Figure 2.15 Experimental setup (Guoyi Hou, 2021)

Research on the impact of various fibre orientation and process parameters like feed rate and spindle speed on the resultant machining force, machining temperature, damage factor and surface roughness were evaluated by Dhiraj Kumar and Suhasini Gururaja. They discovered that when machining at orientation of 0° , 45° , and 15° in dry conditions particularly, the cutting temperature recorded was higher than glass transition glass temperature (T_g) of

matrix. In contrast, for 90° fibre orientation recorded a lower temperature below the T_g at lower spindle speed and feed rate. Furthermore, due to the significant decrease in machining temperature under cryogenic conditions than dry conditions, it is advisable to consider that method. (Dhiraj Kumar, 2020) The figure 2.15 below shows the temperature difference between cryogenic conditions and dry conditions.

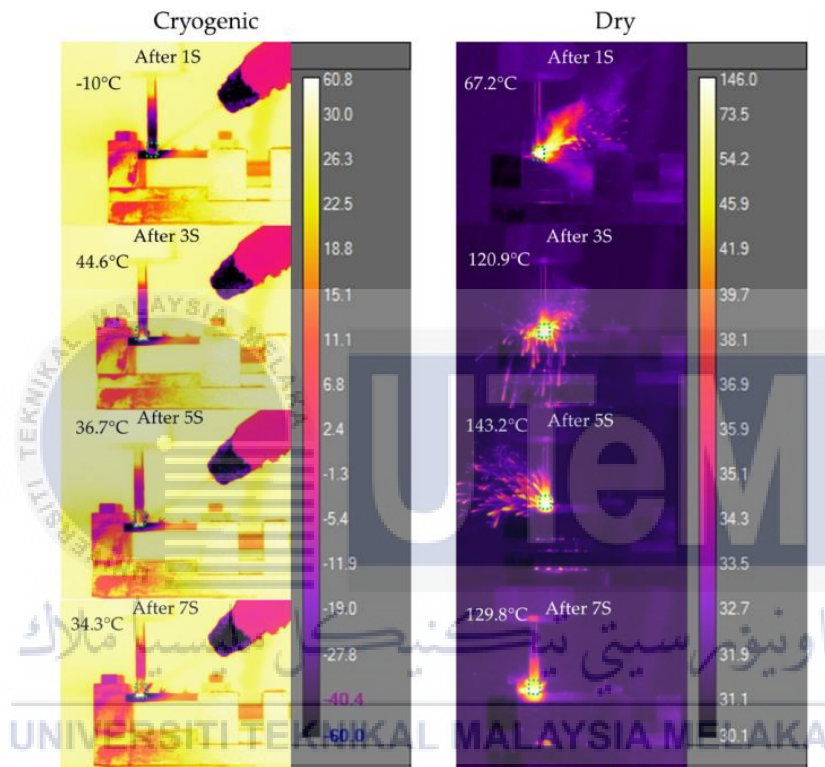


Figure 2.16 Cryogenic conditions (left), dry conditions (right) (Dhiraj Kumar, 2020)

CHAPTER 3

METHODOLOGY

3.1 Introduction

This chapter describes the flow of the research in studying the proposed. The focus project is titled 'to determine the effect of the tool geometrical feature in trimming HFRP material'. This research was carried out based on a few stages of experiments which was conducted properly in order to achieve the objectives that being stated. There were few stages of this research methodology.

The primary stage of this research was selection of cutting tool geometry in terms of type, number of flutes and helix angle that was obtained from related journals and article. Moving on to the next stage is conducting the experiment where it includes setting up the thermal camera as well as run the experiment. The third stage is data collection. The data that will be collected are surface roughness value, cutting temperature and chip formation. The final stage is the analysis of data using ANOVA.

3.2 Process flow chart

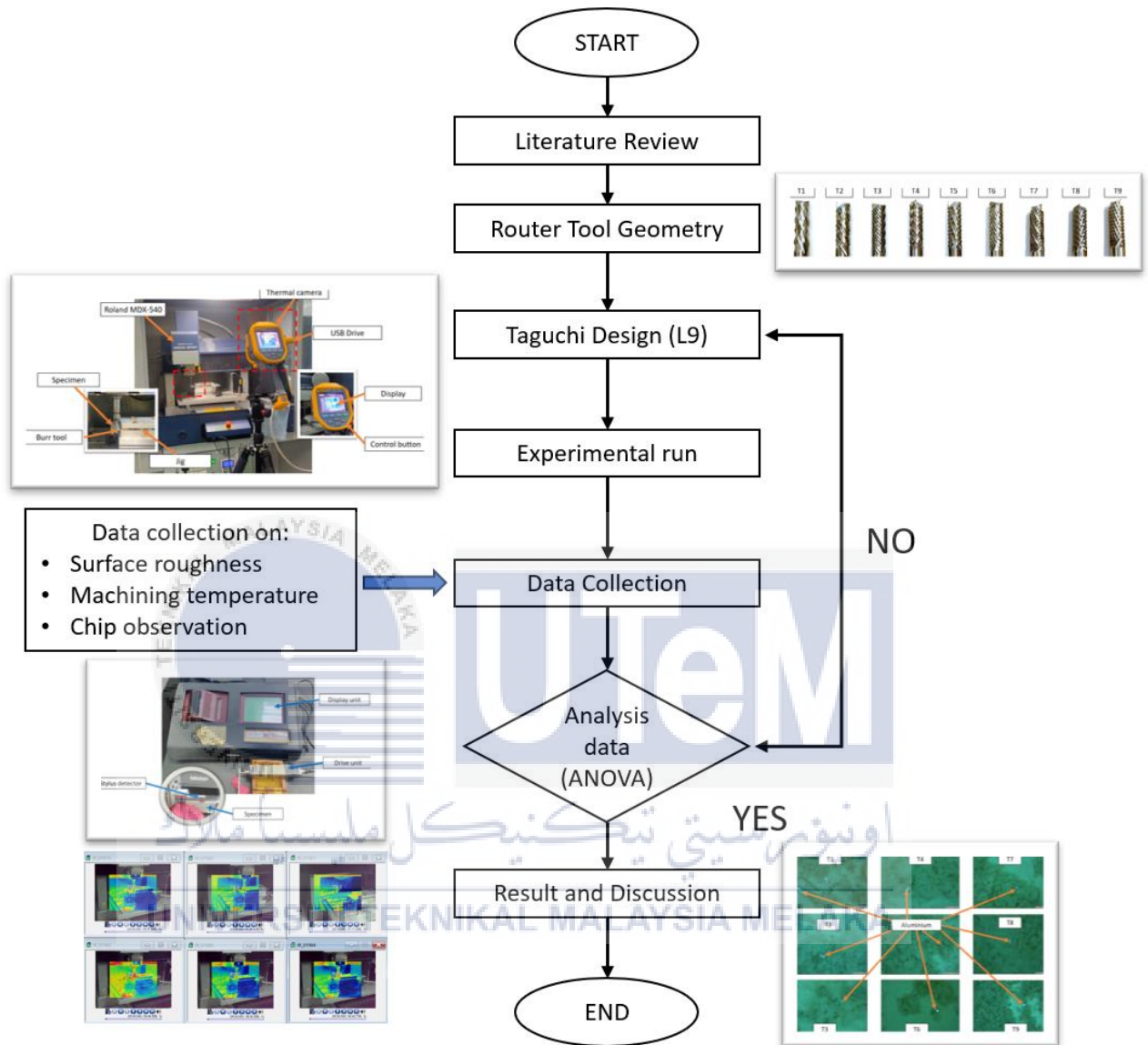


Figure 3.1: Flow of the overall research

3.3 Experimental setup

Figure 3.2 shows the overall experimental setup for trimming HFRP using nine different types of geometrical tools. The HFRP specimen was clamped to the jig and placed on the working table of CNC Router Milling Machine MDX-540. Furthermore, a thermal camera

Fluke ti400 was setup and utilized as it functions to record the temperature of each cutting process.

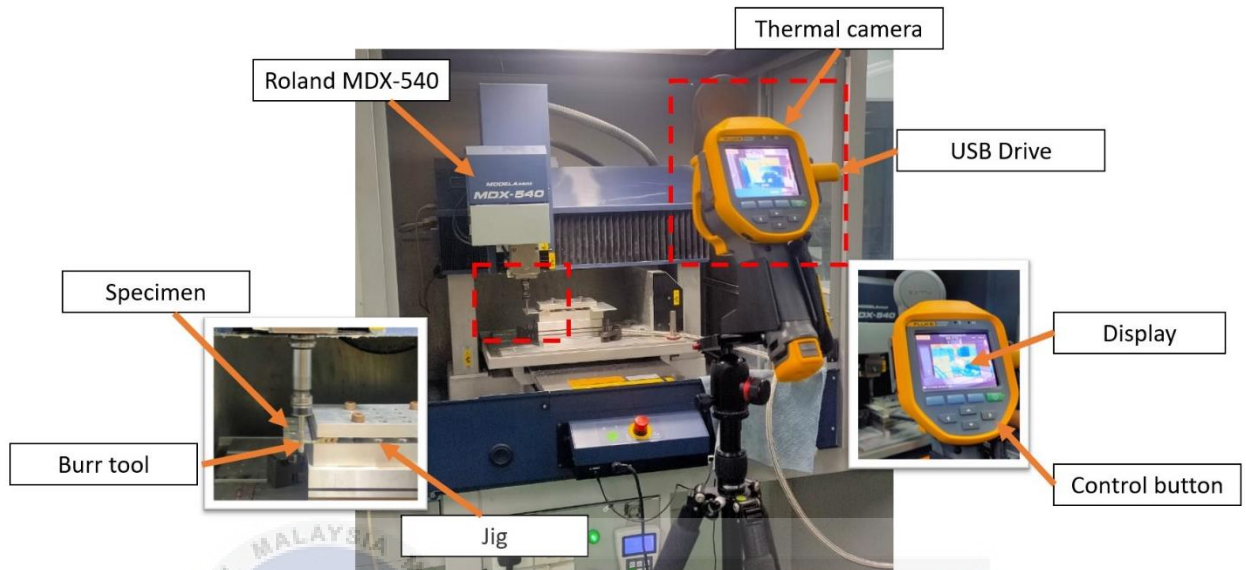


Figure 3.2 Overall Experimental setup

3.4 Materials details

This research is using the actual aerospace HFRP material from a local aerospace composite manufacturing industry (courtesy from ACM Sdn. Bhd.). This material was the actual cut-out from spoiler wing-section in aero-structural component. It has a total of 19 plies of fibre polymer matrix and a layer of aluminium. The orientation of this material is multi-directional. Table 2 indicates the stacking sequence of the HFRP material. Figure 3.3. shows the before and after

Table 2: HFRP stacking direction configuration.

Ply or part number	ORIENTATION
P1	0°/90°
P2	0°/90°
P3	0°/90°
P4	0°/90°
P5	+/- 45°
P6	0°/90°
P7	0°/90°
P8	0°/90°
P9	0°/90°
P10	+/- 45°
P11	0°/90°
P12	0°/90°
P13	0°/90°
P14	0°/90°
P15	+/- 45°
P16	+/- 45°
P17	0°/90°
P18	0°/90°
P19	0°/90°

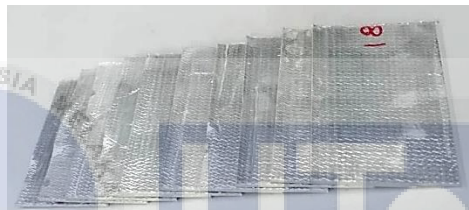


Figure 3.3: The HFRP panel were cut into smaller pieces for the experiment.

3.5 Tool materials

The edge trimming of HFRP composite material was done using uncoated tungsten carbide routers with a 6.35 mm diameter supplied by Everttools Industrial Supply Sdn. Bhd. These tools were specified for trimming composite materials. All of the tools had the same length of 75 mm. The cutter length of the tools was constant for all, which was 20 mm. The helix angle for the right and left side as well as the number of flutes were chosen to be investigated. Figure 3.4, Table 3, and Table 4 indicated the router tools and their details.

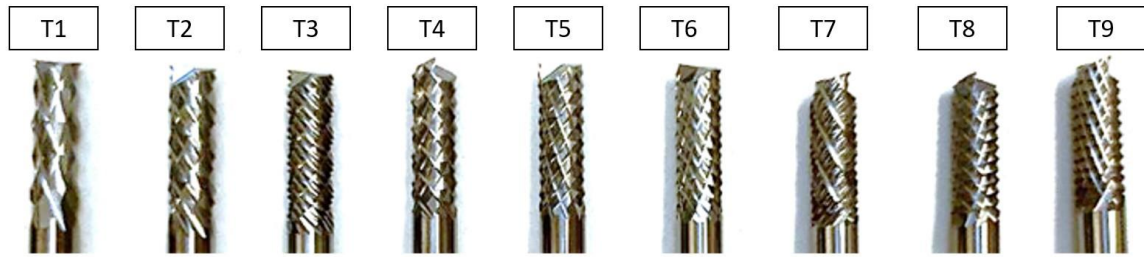


Figure 3.4: Router tools

Table 3: Router design details

Tool geometry	Details
Diameter	6.35mm
No. of flute (Right)	6, 10, 14
No. of flute (Left)	6, 10, 14
Helix angle (Right)	20, 30, 40
Helix angle (Left)	20, 30, 40
Tool length	75mm

UNIVERSITI TEKNIKAL MALAYSIA MELAKA
 اونیورسیتی تکنیکل ملیسیا ملاک
 UNIVERSITI TEKNIKAL MALAYSIA MELAKA

Table 4 : Taguchi L9 experimental matrix

No	No. of flute		Helix angle	
	Right	Left	Right	Left
1	6	6	20	20
2	6	10	30	30
3	6	14	40	40
4	10	6	30	40
5	10	10	40	20
6	10	14	20	30

7	14	6	40	30
8	14	10	20	40
9	14	14	30	20

3.6 Specifications of machine

The trimming operation on composite material was performed on router Roland MDX-540 (Figure 3.5). Table 5 indicates the operating conditions of the router.

Table 5: The operating conditions of the machine

PARAMETERS	SPECIFICATIONS
Max Spindle Speed	12000 rpm
Max Horsepower	15 HP
Max Feed Rate	53.3 m/min
Maximum x-axis Travel Distance	400 mm
Maximum y-axis Travel Distance	400 mm
Maximum z-axis Travel Distance	100 mm



Figure 3.5: Roland MDX-540.

3.7 Machining parameters

Constant cutting conditions, cutting speed (V_C) and spindle speed were applied for all the tools. Cutting speed of 150m/min and spindle speed of 7518 rev/min were used for the trimming operation of HFRP.

3.8 Jig preparation

Before starting the machining of HFRP, it was crucial to prepare the jig and fixture. In order to achieve a satisfactory result from the HFRP machining analysis, the jig and fixture were also very important. The HFRP specimen would vibrate while being machined if the jig does not lock it properly. Figure 3.6 and Figure 3.7 showed the jig that will be used in this experiment.

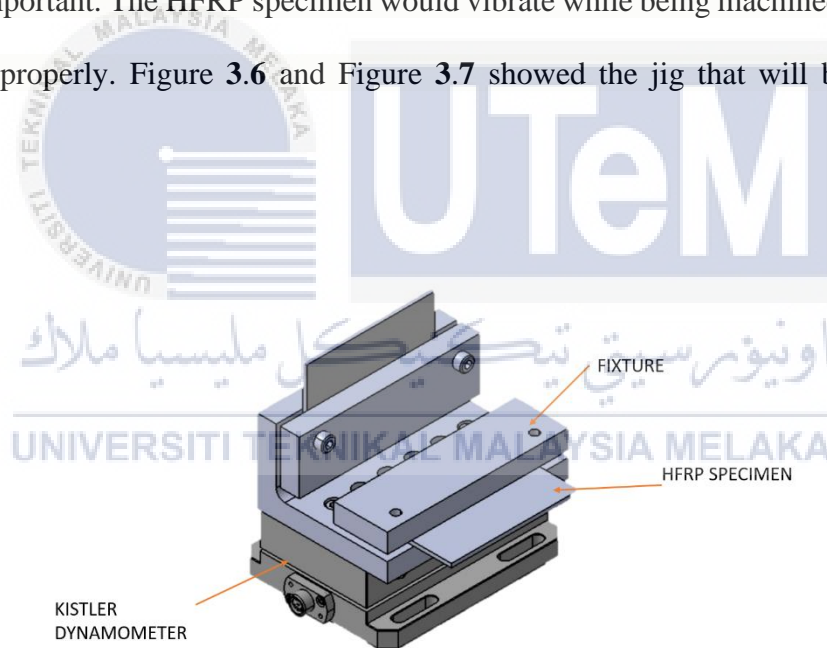


Figure 3.6: Details of the jig



Figure 3.7: Jig to hold the specimens.

3.9 Surface roughness

Mitutoyo SJ-310 (Figure 3.8) was used to measure the surface quality of the trimmed component. This tester was chosen due to its sensitivity that can measure up to $0.01 \mu\text{m}$. Arithmetic average (R_a) was used as the surface roughness measurement. The surface roughness of the machine component was evaluated in longitudinal and transverse measurement direction. The test was assessed with three measurements (start, middle and end) as in Figure 3.8 each place on each machined surface resulting to nine reading per surface. The travel distance of the stylus was set to 5mm and 0.32mm for every longitudinal and transverse measurement direction respectively.

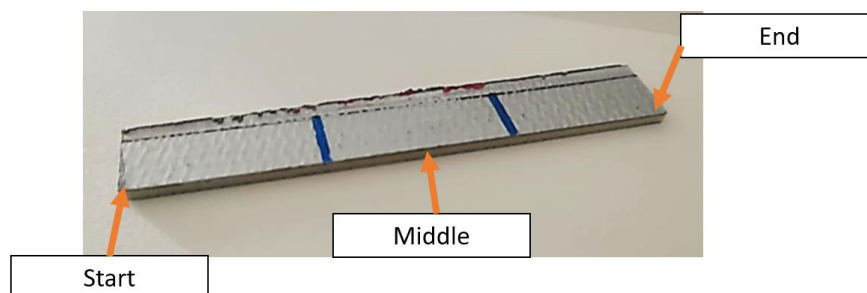


Figure 3.8 HFRP Panel

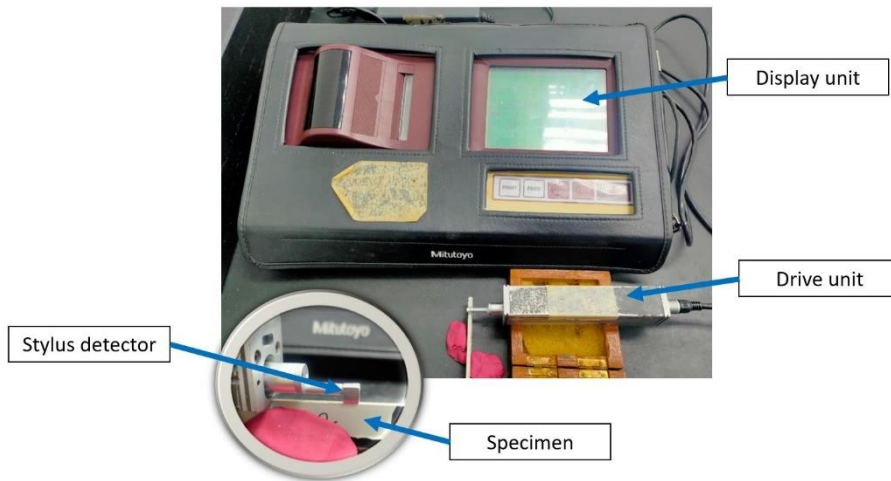


Figure 3.9: SJ-310 for measuring surface roughness.

3.10 Cutting Temperature

Fluke ti400 thermal camera was utilized to obtain the cutting temperature by recording the whole machining process. Figure 3.10 showed some of cutting temperature recordings obtained from the thermal camera.

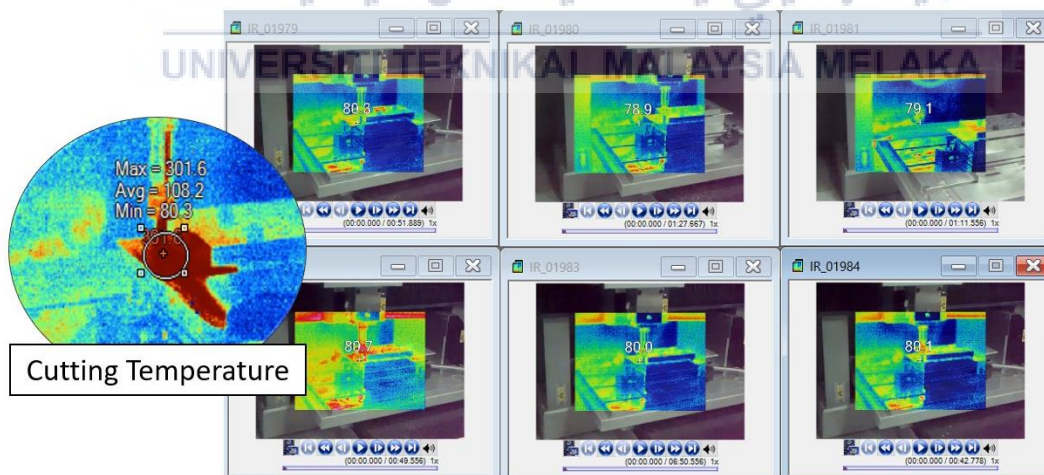


Figure 3.10 Cutting Temperature Recordings

However, the recording from the thermal camera needs to use an additional software known as Fluke SmartView to view it. The first step to open the recording files was transferring the

recording into laptop. Then, open the SmartView Software, click on File and Open... as shown in Figure 3.11 to select the recording file from the existing file.

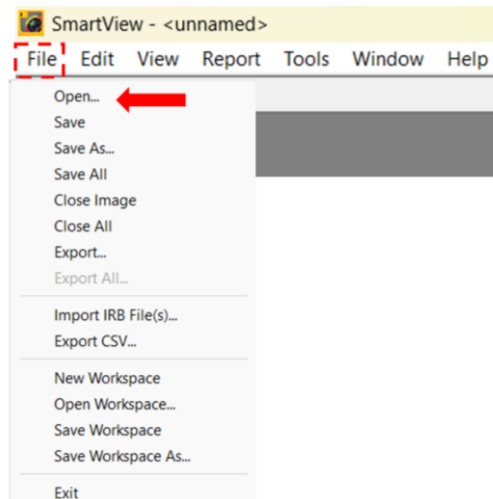


Figure 3.11 Opening the Recording from Existing File.

After that, click on the rainbow colour icon (Figure 3.12) to open the settings. Then, the point of temperature reading was adjusted to hot cursor (Figure 3.13) which it automatic detect the highest temperature along the cutting process. So, it was an easy and accurate ways to obtain the cutting temperature.

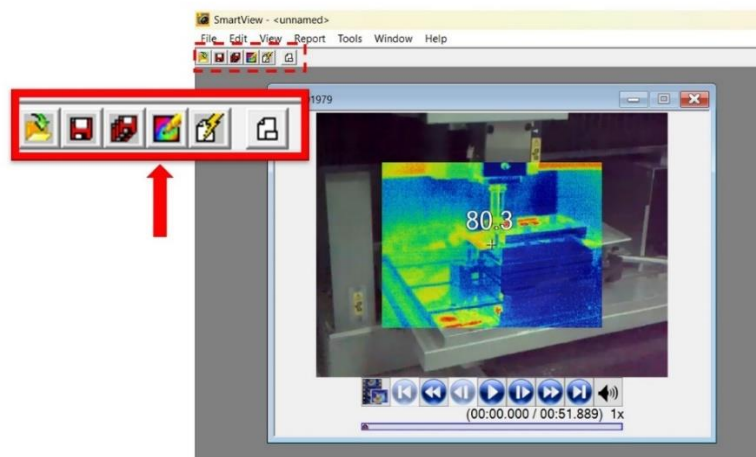


Figure 3.12 Step to analysed cutting temperature.

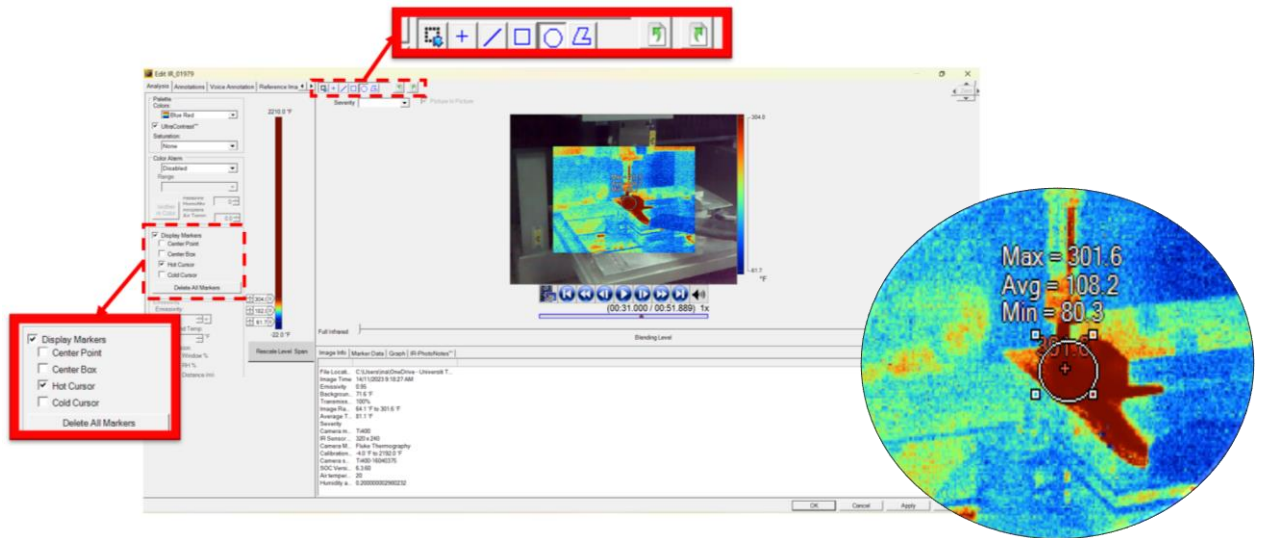
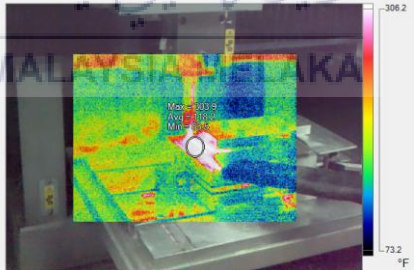
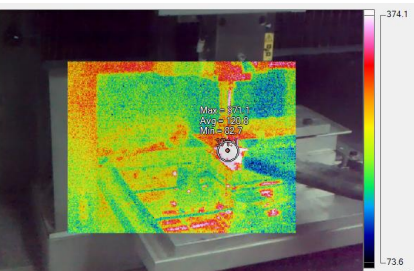
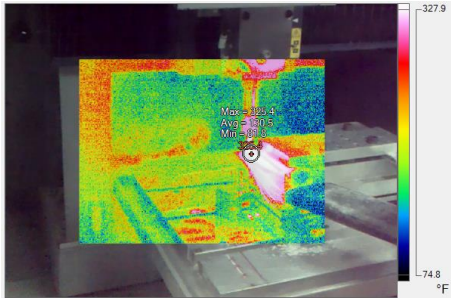


Figure 3.13 Fluke SmartView setting.

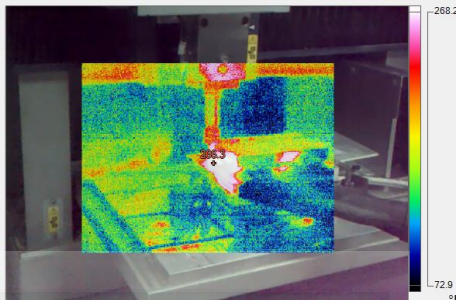
The process was repeat for all recording and the maximum temperature for all runs were tabulated as in Table 6 below.

Table 6 Maximum Cutting Temperature for All Run

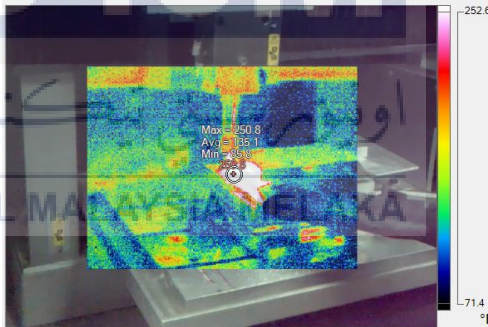
Tool	Maximum temperature (°F)
	 <p style="text-align: center;">303.9</p>
	 <p style="text-align: center;">371.1</p>



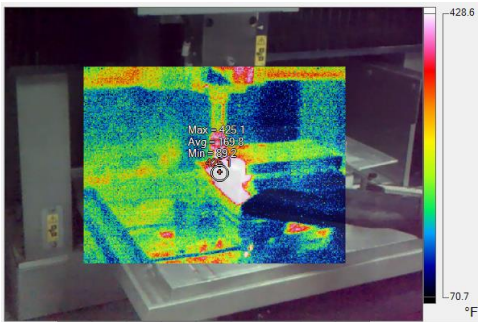
325.4



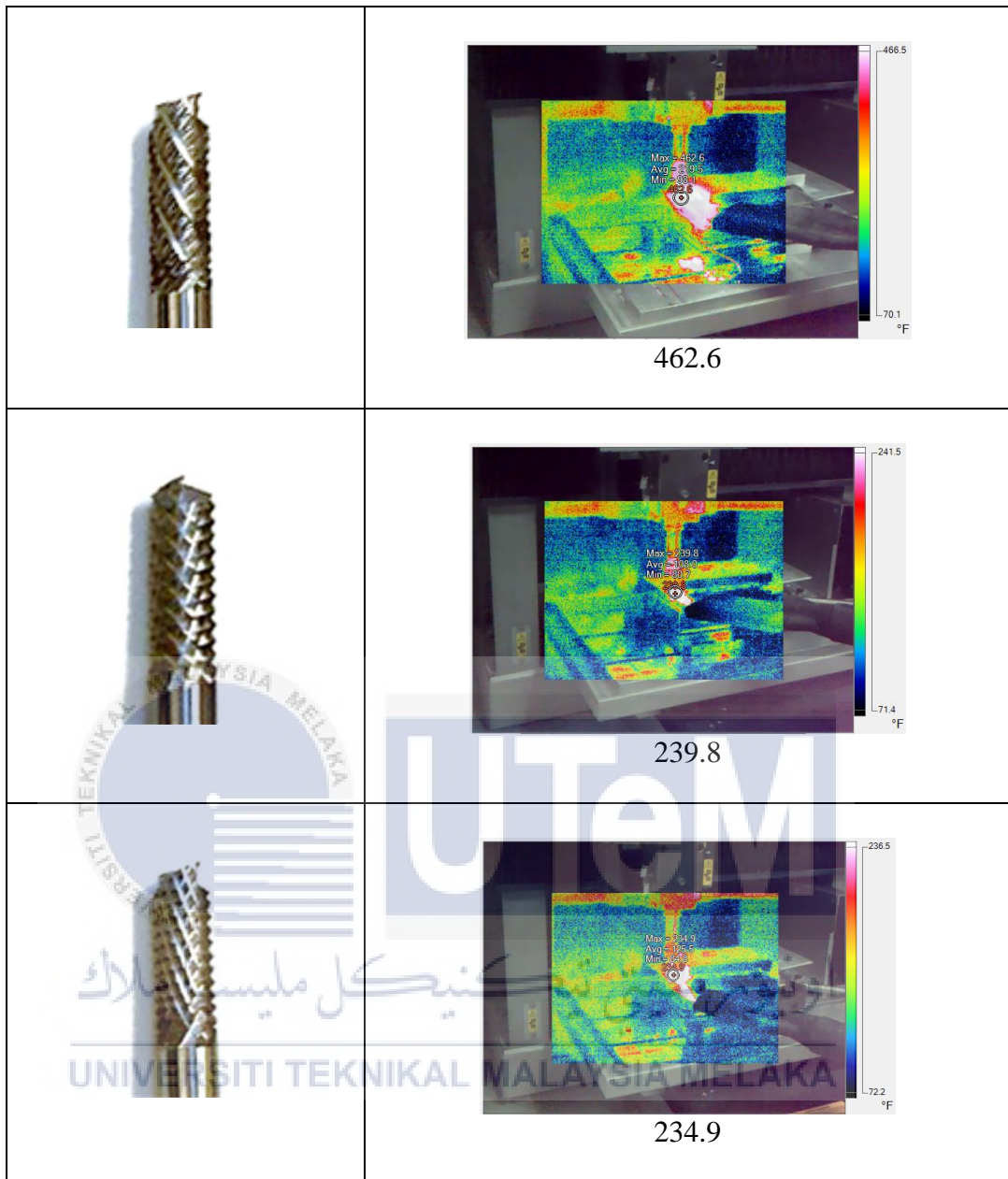
266.3



250.8



425.1



3.11 Chip Observation

Chip that were produced during trimming process were observed under Nikon MM-800 microscope (Figure 3.14). with the ability to zoom until 100x magnification maximum, helps to display a clear results of tool damages. The images taken by the microscope were

processed by E-Max software. This software offers a thorough image analysis for examining the structure and magnitude of visual information.



Figure 3.14 Nikon MM-800



CHAPTER 4

RESULTS

4.1 Surface Roughness

4.1.1 Down-milling

The surface roughness results for down-milling that measured for both directions, transverse and longitudinal were shown in Table 7 And Table 8, from the results obtained, surface roughness for transverse direction in Table 7 and Figure 4.1, tool 9 with the 14 number of teeth for both left and right, 20° and 30° for right and left helix angle respectively contributes the highest value of surface roughness which was 1.80µm. in contrast tool 6 with 10 and 14 number of flute and 20° and 30° helix angle for right and left side respectively contributes the lowest surface roughness value which was 0.95 µm. On the other hand, surface roughness value for longitudinal direction were shown in Table 8 and Figure 4.2, the same tool 9 represent the highest Ra value with 6.35 µm and tool 3 represent the lowest value with 2.67µm.

This is due to the presence of sharp cutting edge of pyramid shape tooth profile. This is confirmed by other studies that had observed that the number of flutes with the presence of pyramidal cutting edge highly influenced the increasing result of surface roughness value. (Rangasamy Prakash, 2016). Moreover, Tool 6 and tool 3 have the lowest surface roughness for transverse and longitudinal direction because their cutting temperature ($T_6 = 425.1$ and $T_3 = 325.4$) were greater than tool 9 (234.9) which it could soften the HFRP matrix and make it easier to cut and lead to a smoother surface finish compared to tool 9.

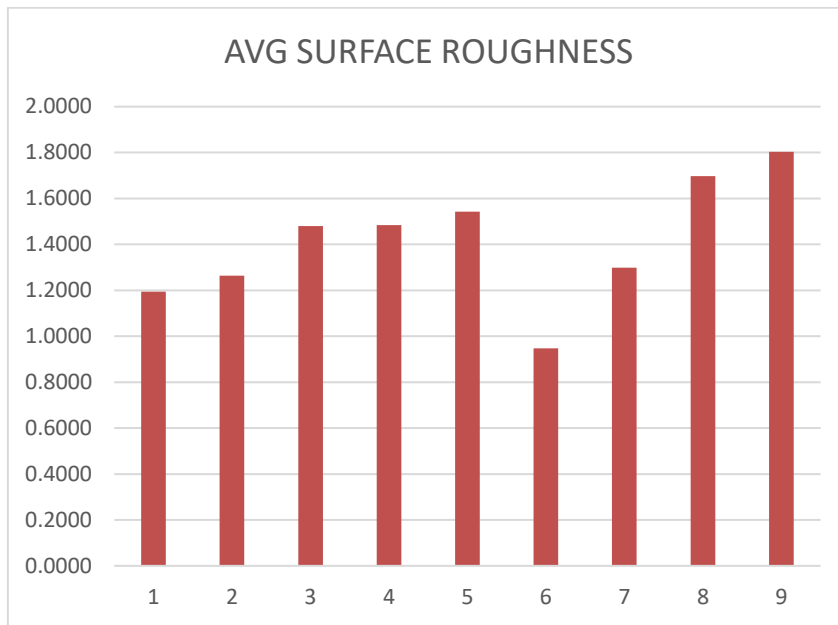


Figure 4.1 Average Surface Roughness for transverse direction

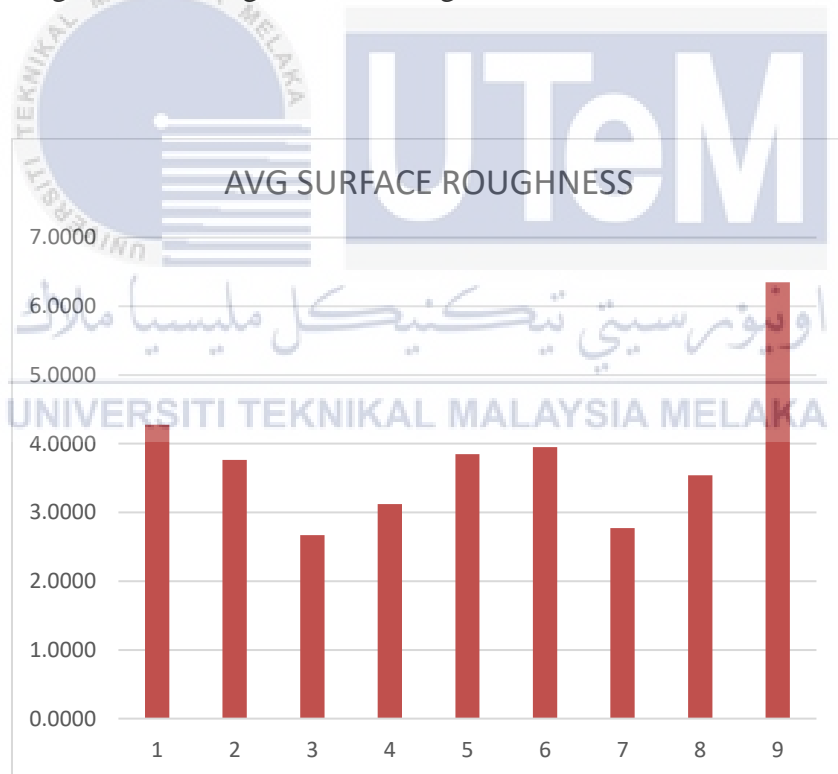


Figure 4.2 Average Surface Roughness for longitudinal direction

Table 7 Average surface roughness for transverse direction

TOOL NUMBER	START				MIDDLE				END				AVG SURFACE ROUGHNESS
	1	2	3	AVG	1	2	3	AVG	1	2	3	AVG	
T1	1.69	1.2	0.84	1.243	0.9	1.17	1.76	1.28	1.08	1.25	0.86	1.06	1.19
T2	1.21	1.09	0.67	0.990	0.8	0.94	1.82	1.19	2.02	1.31	1.51	1.61	1.26
T3	1.23	1.78	1.24	1.417	1.66	0.88	1.5	1.35	1.53	1.55	1.95	1.68	1.48
T4	1.9	1.67	1.62	1.730	1.75	0.83	1.46	1.35	1.24	1.23	1.66	1.38	1.48
T5	1.96	1.66	1.8	1.807	1.25	1.74	2.09	1.69	0.159	1.6	1.62	1.13	1.54
T6	1.37	1.3	0.93	1.200	0.87	0.66	0.75	0.76	0.65	0.94	1.06	0.88	0.95
T7	1.12	0.87	1.67	1.220	1.12	1.68	1.61	1.47	1.48	1.35	0.79	1.21	1.30
T8	1.34	1.6	1.38	1.440	1.68	1.46	2.78	1.97	1.81	1.68	1.55	1.68	1.70
T9	1.26	1.31	1.29	1.287	1.41	2.02	1.81	1.75	3.5	2.16	1.47	2.38	1.80

Table 8 Average surface roughness for longitudinal direction

TOOL NUMBER	START				MIDDLE				END				AVG SURFACE ROUGHNESS
	1	2	3	AVG	1	2	3	AVG	1	2	3	AVG	
T1	5	4.41	6.6	5.34	3.78	4.31	4.57	4.22	2.14	3.12	4.56	3.27	4.28
T2	4.4	4.75	1.33	3.49	2.37	3.36	2.68	2.80	4.54	5.14	5.31	5.00	3.76
T3	2.77	2.69	2.13	2.53	2.97	2.89	2.01	2.62	3.84	2.34	2.39	2.86	2.67
T4	3.6	4.55	4.23	4.13	4.98	2.07	2.19	3.08	3.64	1.47	1.36	2.16	3.12
T5	2.02	2.55	2.15	2.24	2.89	5.87	6.02	4.93	4.97	4.51	3.66	4.38	3.85
T6	3.63	1.73	4.35	3.24	5.78	2.1	3.03	3.64	4.91	4.72	5.29	4.97	3.95
T7	2.32	2.49	1.32	2.04	2.92	3.73	5.05	3.90	3.97	1.99	1.18	2.38	2.77
T8	1.28	2.5	5.2	2.99	1.58	2.69	5.43	3.23	5.31	3.86	4.01	4.39	3.54
T9	7.67	7.12	7.39	7.39	5.98	5.03	6.37	5.79	7.21	4.73	5.64	5.86	6.35

4.1.2 Up-milling

The surface roughness results for down-milling that measured for both directions, transverse and longitudinal were shown in table 9 And table 10, from the results obtained, surface roughness for transverse direction (Figure 4.3 and Table 9), tool 3 with the 6 and 14 number of teeth for both left and right respectively, 40° for both right and left helix angle contributes the highest value of surface roughness which was 1.41 μm . In contrast tool 6 with 10 and 14 number of flute and 20° and 30° helix angle for right and left side respectively contributes the lowest surface roughness value which was 0.61 μm . On the other hand, surface roughness value for longitudinal direction were shown in Table 10 and Figure 4.4 tool 9 represent the highest Ra value with 5.75 μm and tool 6 represent the lowest value with 1.37 μm .

This is because tool 6 has a higher cutting temperature compared to tool 3 and tool 9. Temperature can affect the mechanical properties of a material including HFRP. High temperature obviously affects the development of chips and subsurface damage as the resin will become softer and lose some of its strength. (Guoyi Hou, 2021). Thus, the HFRP becomes easier to cut and has a better surface roughness.

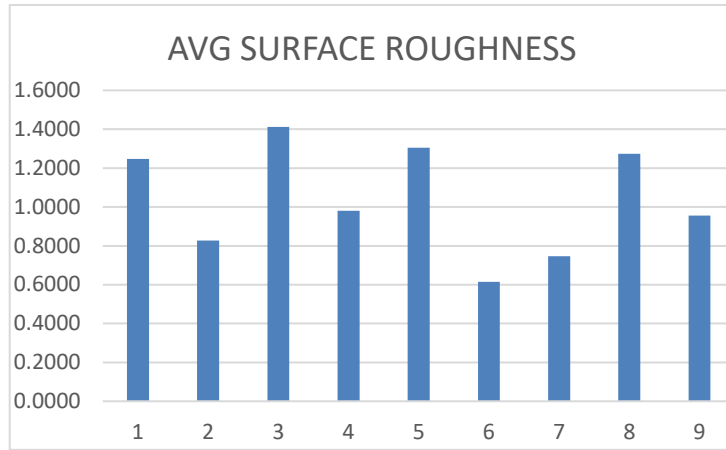


Figure 4.3 Average Surface Roughness for transverse direction

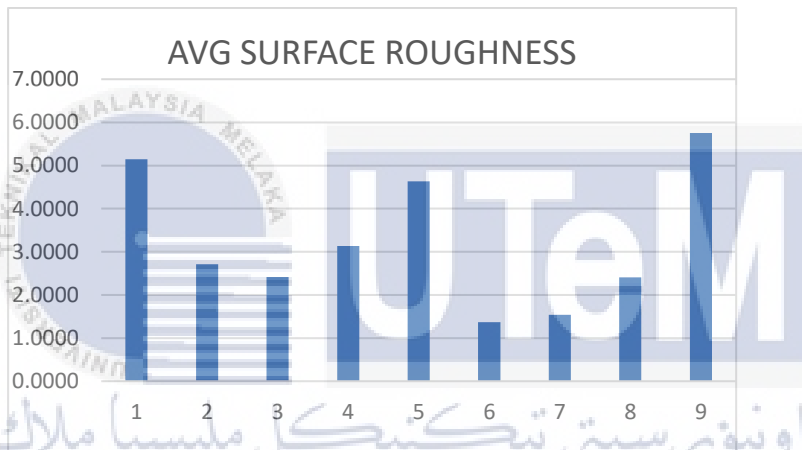


Figure 4.4 Average Surface Roughness for Longitudinal direction

UNIVERSITI TEKNIKAL MALAYSIA MELAKA

Table 9 Average surface roughness for transverse direction

TOOL NUMBER	START				MIDDLE				END				AVG SURFACE ROUGHNESS
	1	2	3	AVG	1	2	3	AVG	1	2	3	AVG	
T1	1.01	1.55	1.09	1.22	1.36	1.67	1.19	1.41	1.5	0.87	0.99	1.12	1.25
T2	0.6	0.28	0.76	0.55	0.49	0.94	1.35	0.93	0.93	1.34	0.75	1.01	0.83
T3	1.15	1.65	1.22	1.34	1.49	1.73	1.19	1.47	1.66	1.31	1.31	1.43	1.41
T4	0.97	1.37	1.06	1.13	0.74	0.79	0.9	0.81	1.34	1.01	0.64	1.00	0.98
T5	1.87	1.34	1.61	1.61	1.27	1.33	0.98	1.19	1.32	0.79	1.24	1.12	1.31
T6	0.26	0.47	0.48	0.40	0.66	0.42	1.17	0.75	0.74	0.74	0.59	0.69	0.61
T7	0.41	0.48	0.86	0.58	0.51	1.16	0.66	0.78	0.77	1.09	0.78	0.88	0.75
T8	0.91	0.8	1.32	1.01	1.57	1.5	1.42	1.50	1.19	1.48	1.27	1.31	1.27
T9	1.08	1.06	0.81	0.98	0.8	0.75	1.03	0.86	0.78	1.08	1.21	1.02	0.96

Table 10 Average surface roughness for longitudinal direction

TOOL NUMBER	START				MIDDLE				END				AVG SURFACE ROUGHNESS
	1	2	3	AVG	1	2	3	AVG	1	2	3	AVG	
T1	5.78	7.16	5.61	6.18	5.34	4.55	5.15	5.01	3.68	5.04	3.98	4.23	5.14
T2	2.35	1.31	2.47	2.04	1.87	2.32	4.71	2.97	3.77	2.02	3.57	3.12	2.71
T3	2.67	3.54	2.2	2.80	1.87	2.18	1.99	2.01	2.46	2.24	2.59	2.43	2.42
T4	4.2	2.53	3.09	3.27	3.59	2.85	2.52	2.99	3.47	3.71	2.22	3.13	3.13
T5	6.01	6.84	4.18	5.68	3.39	5.66	5.71	4.92	2.15	4.07	3.71	3.31	4.64
T6	0.86	0.86	0.63	0.78	0.79	0.84	1.71	1.11	1.9	0.63	4.07	2.20	1.37
T7	2.18	0.62	2.14	1.65	2.03	1.91	1.12	1.69	1.86	1.37	0.63	1.29	1.54
T8	1.76	1.72	2.14	1.87	2.18	2.53	2.2	2.30	3.04	2.56	3.56	3.05	2.41
T9	3.39	7.43	8.18	6.33	6.33	5.23	6.89	6.15	4.09	4.59	5.64	4.77	5.75

4.1.3 Comparison

The blue bar represents the value of surface roughness for up-milling meanwhile for the red bar represents the surface roughness value for down-milling. Based on the findings (Figure 4.5 and Figure 4.6), surface roughness is lower during up-milling than during down-milling. The cutting force is applied against the movement of the workpiece when up-milling. The material is pushed away from the cutting tool as a consequence of the cutting operation, which may help to lessen the amount of material that is left on the surface of the workpiece. A smooth surface finish could be the outcome of this. In contrast, the cutting force in down-milling is applied in the same direction as the workpiece's motion. This cutting motion may leave more material on the surface of the workpiece by drawing the material into the cutting tool. This could lead to a harsher surface finish.

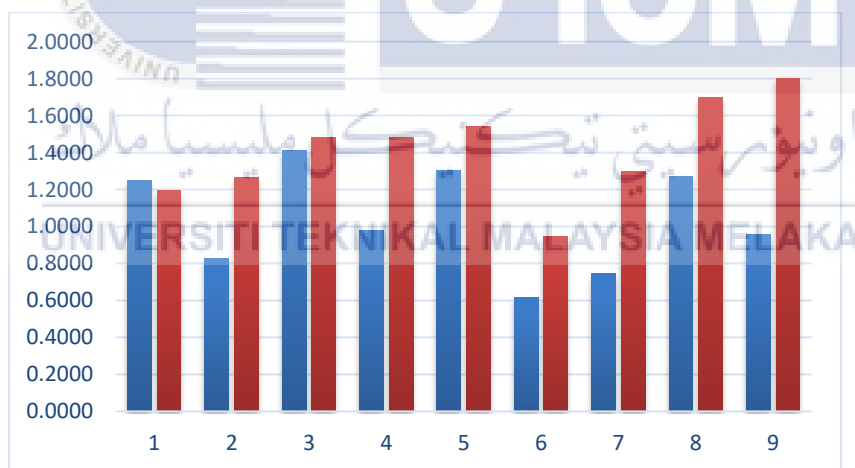


Figure 4.5 Comparison of Average Surface Roughness for transverse direction for down milling and up milling

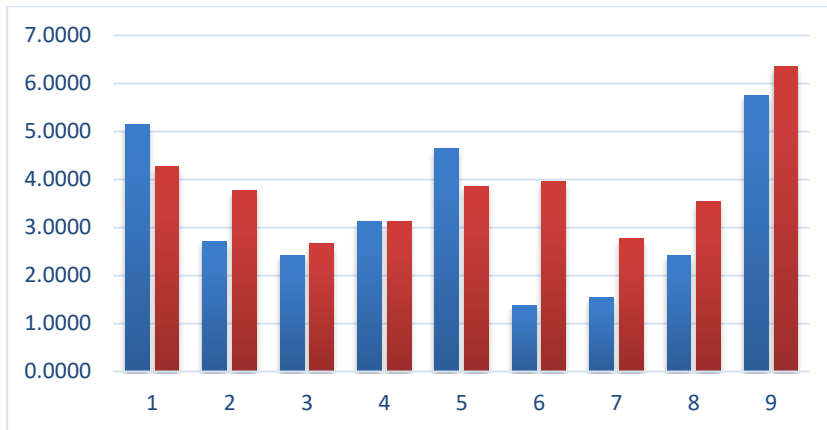


Figure 4.6 Comparison of Average Surface Roughness for longitudinal direction for down milling and up milling

4.2 Cutting temperature

The cutting temperature data that were obtained during the trimming process was represented in Figure 4.9 below. It shows that the heat exerted during trimming of HFRP for Tool 7 was the highest which was 462.6°F followed by Tool 6 (425.1°F), tool 2 (371.1°F), tool 3 (325.4°F), tool 1 (303.9°F), tool 4 (266.3°F), tool 5 (250.8°F), tool 8 (239.8°F) and tool 9 (234.9°F).

The highest (tool 7) and lowest (tool 9) temperature shared the same number of flutes on the right side which was 14 teeth but differ for the other side which were 6 and 14 teeth respectively. Theoretically, high number of teeth resulting in a lower feed per tooth based on the formula of feed per tooth:

$$f_z = \frac{V_f}{n \times Z_c}$$

The tool temperature is influenced by the feed per tooth, f_z . (Arquimedes Castillo-Morales, 2021). For this experiment, feed rate, V_f , and spindle speed, n , were set as a constant variable at 150 m/min and 7518 rpm. Based on the feed per tooth, f_z formula, number of flutes inversely proportional to feed per tooth. This means the number of flutes increases, the feed per tooth decreases and resulting in hinger temperature. From this statement, tool 9 supposedly had the highest cutting temperature because tool 9 has the highest number of flutes compared to all. This is due to the presence of sharp cutting edges known as pyramidal shape cutting edges that help to easily removed the material without using any extra load needed. Hence why the heat exerted from the cutting process was the lowest. Meanwhile, shape of cutting tool 7 possess more like trapezoidal shape, so, tool 7 needs to provide a higher load to the cutting tool, which led to the highest cutting temperature (Figure 4.8).

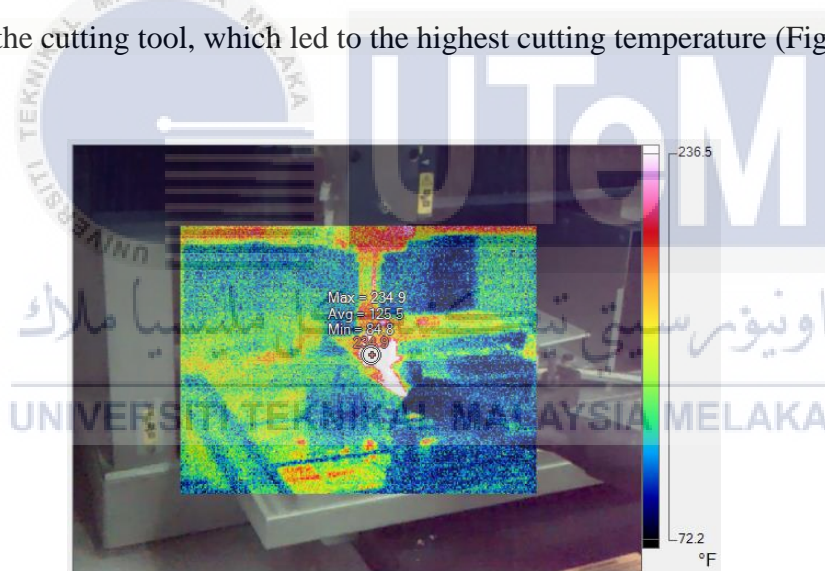


Figure 4.7 Lowest Cutting Temperature

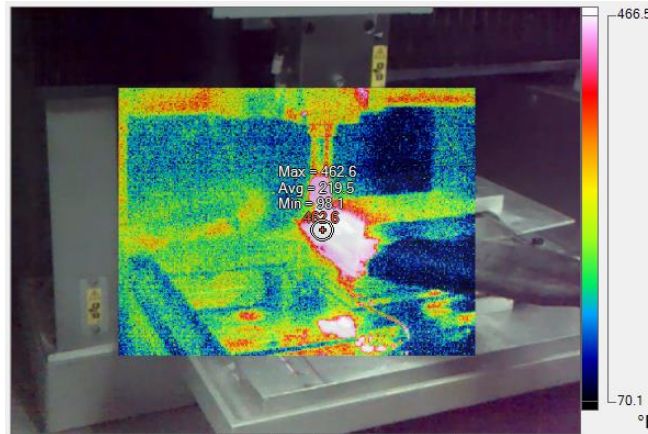


Figure 4.8 Highest Cutting Temperature

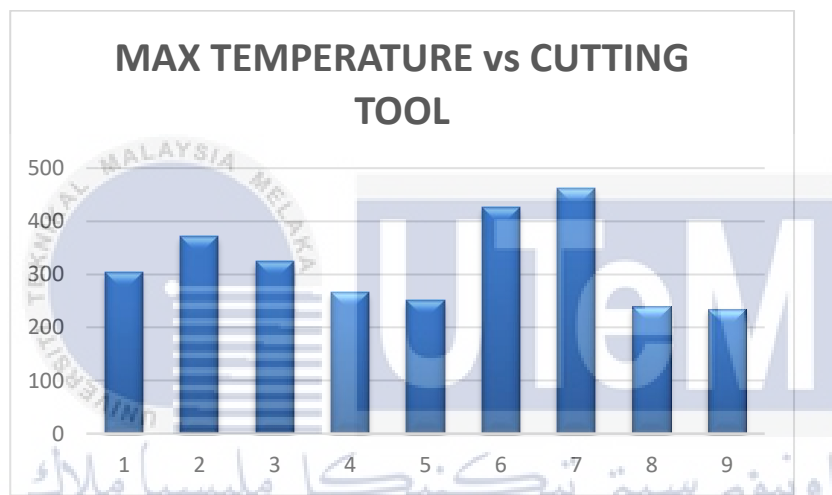


Figure 4.9 Bar Chart of Maximum temperature vs Cutting Tool

4.3 Chip Observation

The chip formation was observed and the results as in Figure 4.10 below. It has been proved that there is aluminium layer in between fibre layer when there was aluminium chip produced when trimming HFRP material. However, the size and shape of the chips were not the same. It is due to the number of flutes and the helix angle. Chips that formed using tool 1 were the most obvious compared to other tools. This is due to the small number of teeth that make the surface contact between cutting edge and the specimen bigger resulting in a bigger chip. Since the fibre in this HFRP material were stacked in the direction of 0° , 45° and 90° , the

chip observation obtained were powdery particles. This was confirmed in research by A.I. Azmi where he found that the chips of fibre and epoxy matrix broke into powdery when cutting at 45° and 90° fibre orientation. (Azmi, 2013)

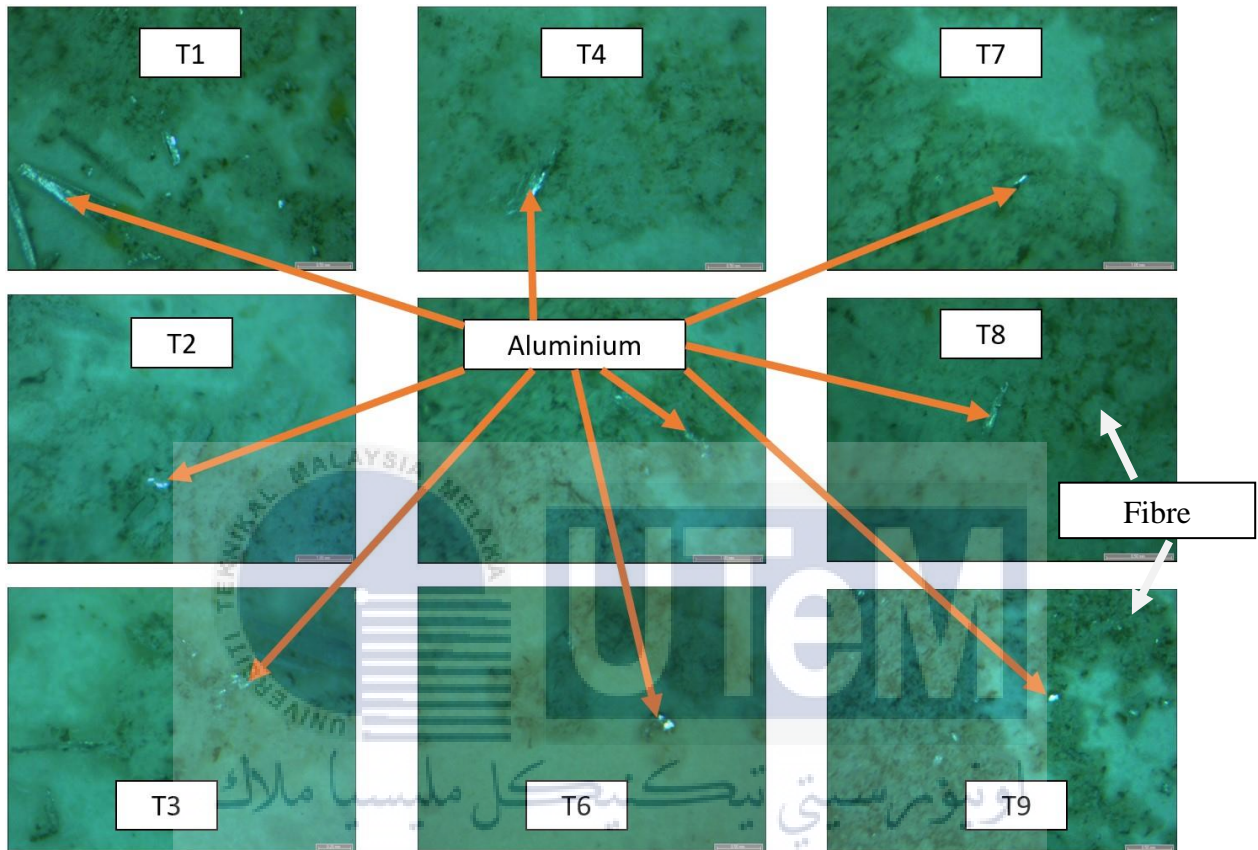


Figure 4.10 Chip formation

4.4 Optimization using Taguchi Method

4.4.1 Signal To Noise Ratio

- a) Taguchi Analysis: Surface Roughness, Ra (upcut) versus No. of Flute (Right), No. of Flute (Left), Helix Angle (Right), Helix Angle (Left)

The goal of this research is to identify the optimum condition for surface roughness when cutting HFRP using nine different cutting geometry. One of the methods used to analyze

data for process optimization uses SN ratio. Figure 4.11 and Table 11 shows the mean of SN ratio for the smaller the better characteristics of surface roughness obtained using Minitab Statistical Software. The slope of the graphs clearly show that left helix angle is the most significant factor, followed by the right helix angle, no. of flute on the right and no. of flute on the left. The optimum condition for upcut is identified by the highest mean SN values. Thus, the optimum condition is no. of flute on the right (10 flute), no. of flute on the left (14 flute), right helix angle (20°) and left helix angle (30°). Moreover, the tabulated data is displayed in Figure 4.12 within the plots of best fit. Although they are not tabulated uniformly, residuals appear to be scattered around the central line. As the residuals are normally distributed, the majority of the data are tallied at the central selection of the overall line.

Table 11 Response Table for Signal to Noise Ratios

Level	NO. OF FLUTE (RIGHT)	NO. OF FLUTE (LEFT)	HELIX ANGLE (RIGHT)	HELIX ANGLE (LEFT)
1	-10.182	-9.296	-8.190	-14.248
2	-8.647	-9.874	-11.257	-5.039
3	-8.862	-8.521	-8.244	-8.405
Delta	1.534	1.353	3.066	9.209
Rank	3	4	2	1

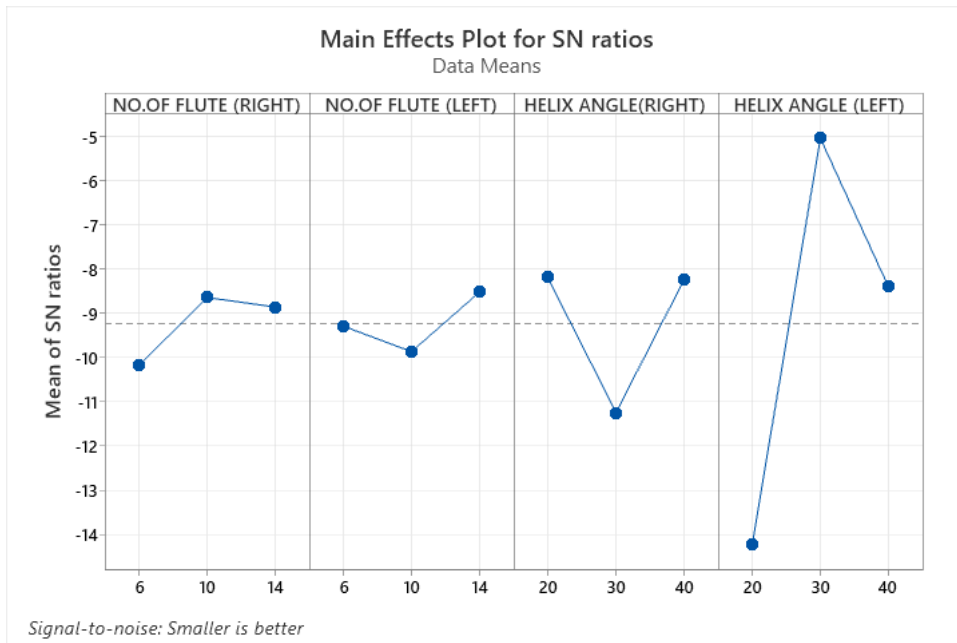


Figure 4.11 Mean of SN ratio for smaller the better characteristics of surface roughness up-milling.

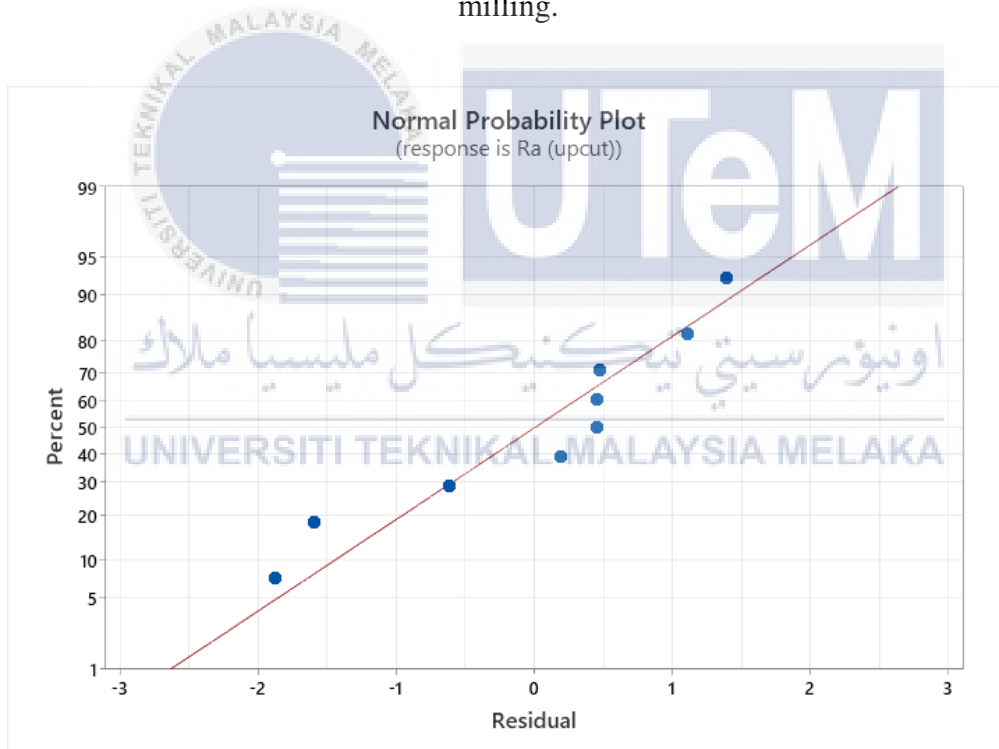


Figure 4.12 Normal Plot of Residuals

b) Taguchi Analysis: Ra (Down cut) Versus No. of Flute (Right), No. of Flute (Left), Helix Angle (Right), Helix Angle (Left)

Figure 4.13 and Table 12 shows the mean of SN ratio for the smaller the better characteristics of surface roughness obtained using Minitab Statistical Software. The slope of the graphs clearly show that left helix angle is the most significant factor, followed by the right helix angle, no. of flute on the left and no. of flute on the right. The optimum condition for upcut is identified by the highest mean SN values. Thus, the optimum condition is no. of flute on the right (6 flute), no. of flute on the left (6 flute), right helix angle (40°) and left helix angle (40°). Furthermore, the tabulated data within the plots of best fit are displayed in Figure 4.14. The residual data are shown to be dispersed not in an even tabulation but rather around the central line. The residuals are normally distributed, and the vast majority of the data are tabulated at the central selection of the overall line.

Table 12 Response Table for Signal to Noise Ratios

Level	NO. OF FLUTE (RIGHT)	NO. OF FLUTE (LEFT)	HELIX ANGLE (RIGHT)	HELIX ANGLE (LEFT)
1	-10.889	-10.457	-11.844	-13.461
2	-11.174	-11.400	-12.485	-10.769
3	-11.966	-12.171	-9.700	-9.799
Delta	1.077	1.714	2.785	3.662
Rank	4	3	2	1

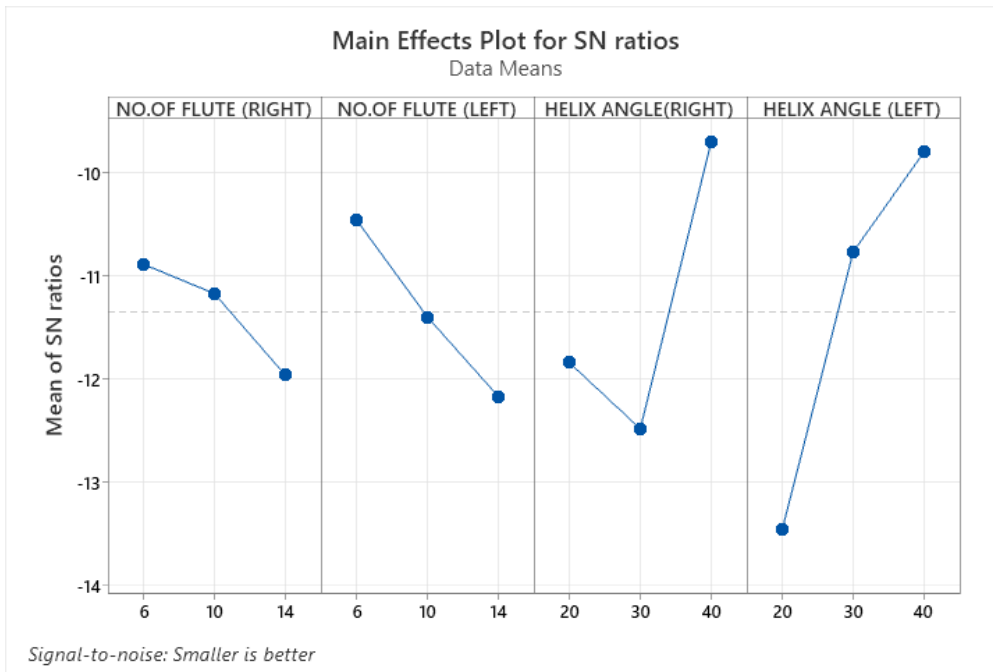


Figure 4.13 Mean of SN ratio for smaller the better characteristics of surface roughness down-milling.

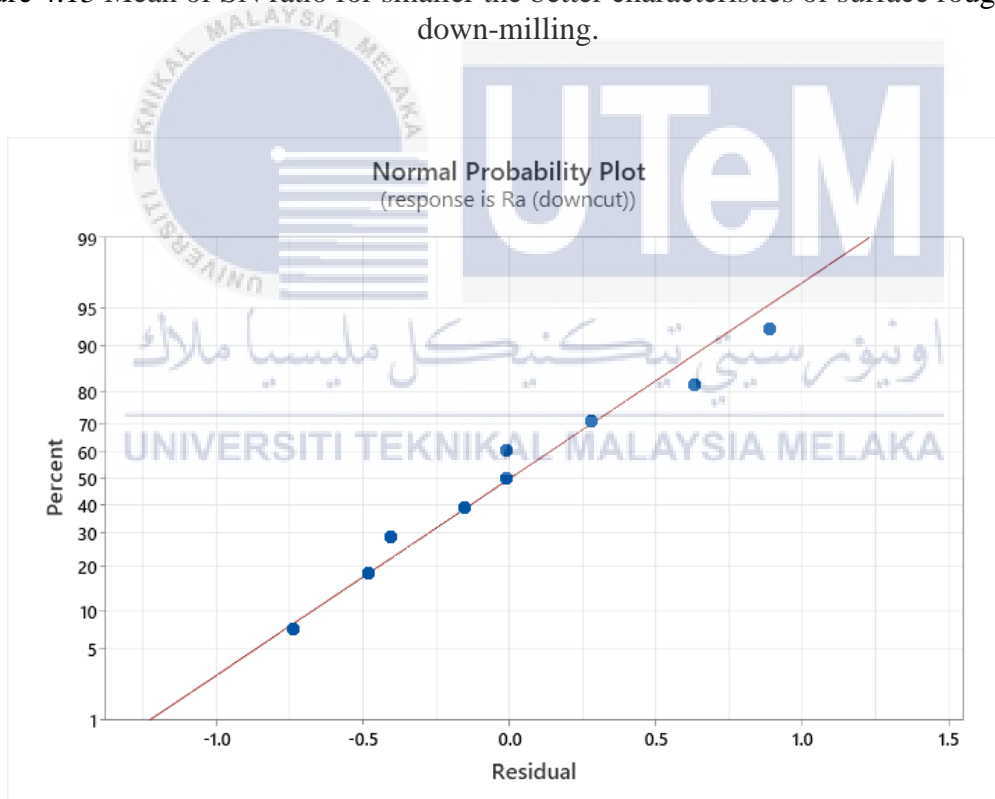


Figure 4.14 Normal Plot of Residuals

c) Taguchi Analysis: Cutting temperature versus No. Of Flute (Right), No. Of Flute (Left), Helix Angle (Right), Helix Angle (Left)

Figure 4.15 shows the mean of SN ratio for the smaller the better characteristics of surface roughness obtained using Minitab Statistical Software. The slope of the graphs clearly show that left helix angle is the most significant factor, followed by the no. of flute on the left, right helix angle and no. of flute on the right. The optimum condition for upcut is identified by the highest mean SN values. Thus, the optimum condition is no. of flute on the right (14 flutes), no. of flute on the left (10 flutes), right helix angle (30°) and left helix angle (20°). Figure 4.16 shows the tubulate data inside the plots of best fit. The residual values are displayed to be distributed around the central line rather than in an even tabulation. Most of the data are tabulated at the overall line's central selection, and the residuals have a normal distribution.

Table 13 Response Table for Signal to Noise Ratios

Level	NO. OF FLUTE (RIGHT)	NO. OF FLUTE (LEFT)	HELIX ANGLE (RIGHT)	HELIX ANGLE (LEFT)
1	-50.43	-50.49	-49.94	-48.35
2	-49.69	-48.99	-49.10	-52.42
3	-49.44	-50.08	-50.51	-48.78
Delta	0.99	1.50	1.41	4.07
Rank	4	2	3	1

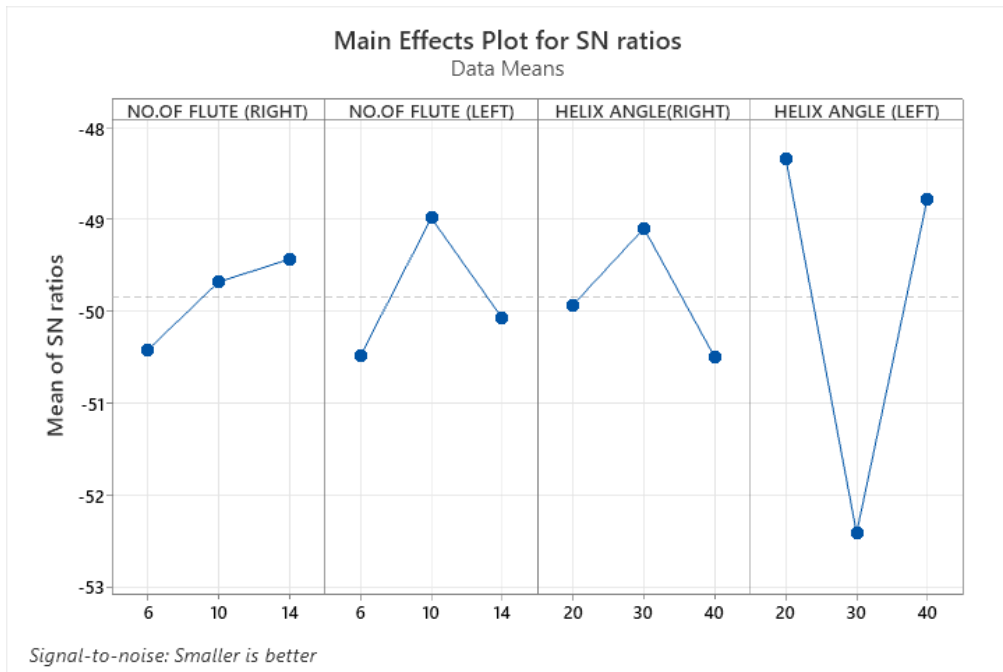


Figure 4.15 Mean of SN ratio for smaller the better characteristics of Temperature.

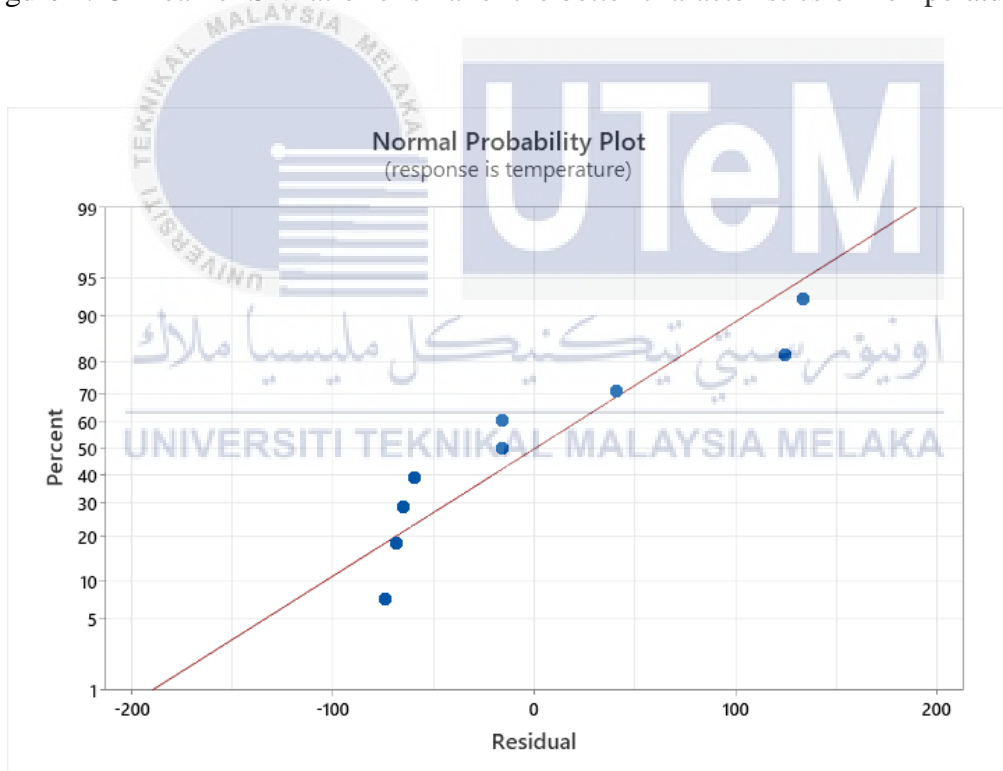


Figure 4.16 Normal Plot of Residuals

CHAPTER 5

CONCLUSION

5.1 Introduction

This chapter examines the findings and recommendations on potential directions for further research regarding the effect of tool geometry features to minimize damage during trimming of Hybrid Fibre Reinforced Polymer (HFRP) material.

5.2 Conclusion

This research highlighted optimizing the cutting geometry, especially the number of flutes and helix angle for both left and right side for edge trimming of Hybrid Fibre Reinforced Polymer. From the findings, this research can be concluded as follows:

1. The tool geometry design (number of flutes and helix angle) significantly affects the surface roughness and machining temperature.
2. The presence of sharp cutting edges (pyramidal shape) makes the trimming process easier and lower temperature. However, the sharp cutting edges leave a harsher cutting surface.
3. The optimum tool geometry for up-milling is the tool that consists of number of flute 10 and 14, helix angle 20° and 30° for right and left side respectively. Meanwhile, for down milling the optimum condition consists of number of flutes 6 and 6, helix angle 40° and 40° for right and left side respectively.

4. Chip formations were highly influenced by the number area of the surface contact between cutting edge and HFRP panel. The larger the surface contact area, the bigger the size of the chip.
5. The ANOVA analysis highlighted that helix angle for left side has the most significant impact for all analysis which are surface roughness for up-milling, surface roughness value for down-milling and also temperature.

5.3 Recommendation and Future Work

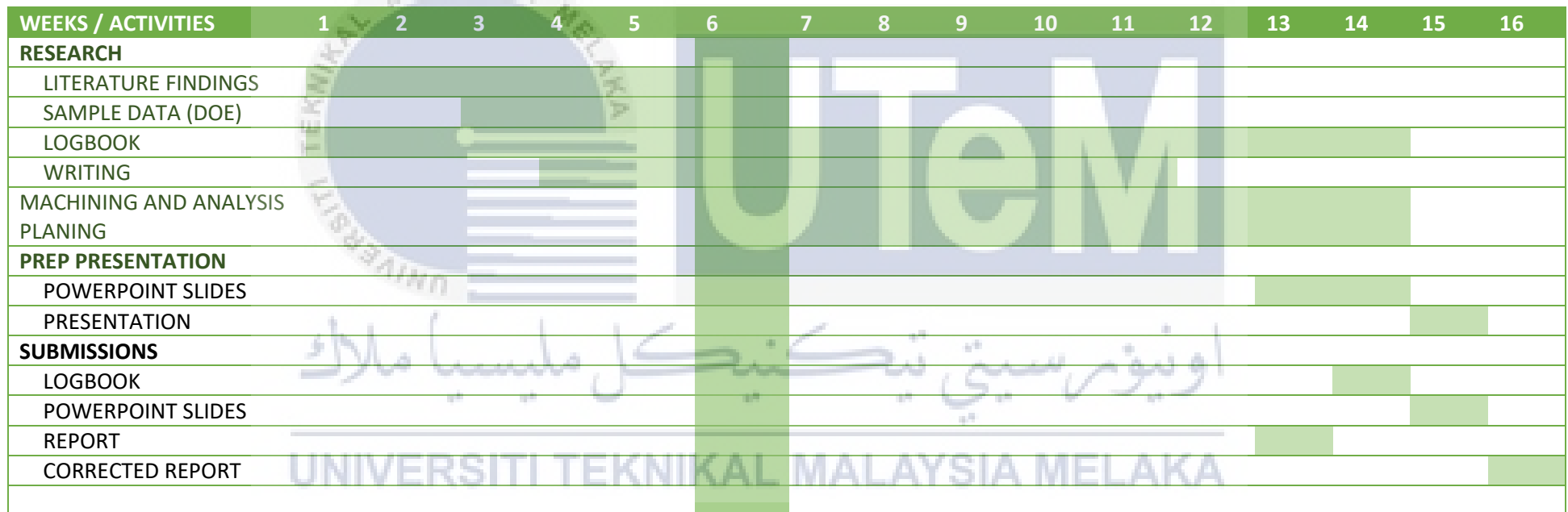
Recommendations for future work are as follows:

1. Use a surface roughness tester that has high sensitivity in order to get the more accurate surface roughness value (Ra).
2. Observation on tool wear and machined surface. Helps to understand more on the correlation between surface roughness and the tool geometry.
3. Analyzing cutting force. Cutting force is a crucial element in machining of composite material as it related to the results of surface quality as well as cutting temperature.
4. Use a microscope with high magnification such as scanning electron micrograph to get better and clear observation on the tool wear and machined surface.

APPENDICES

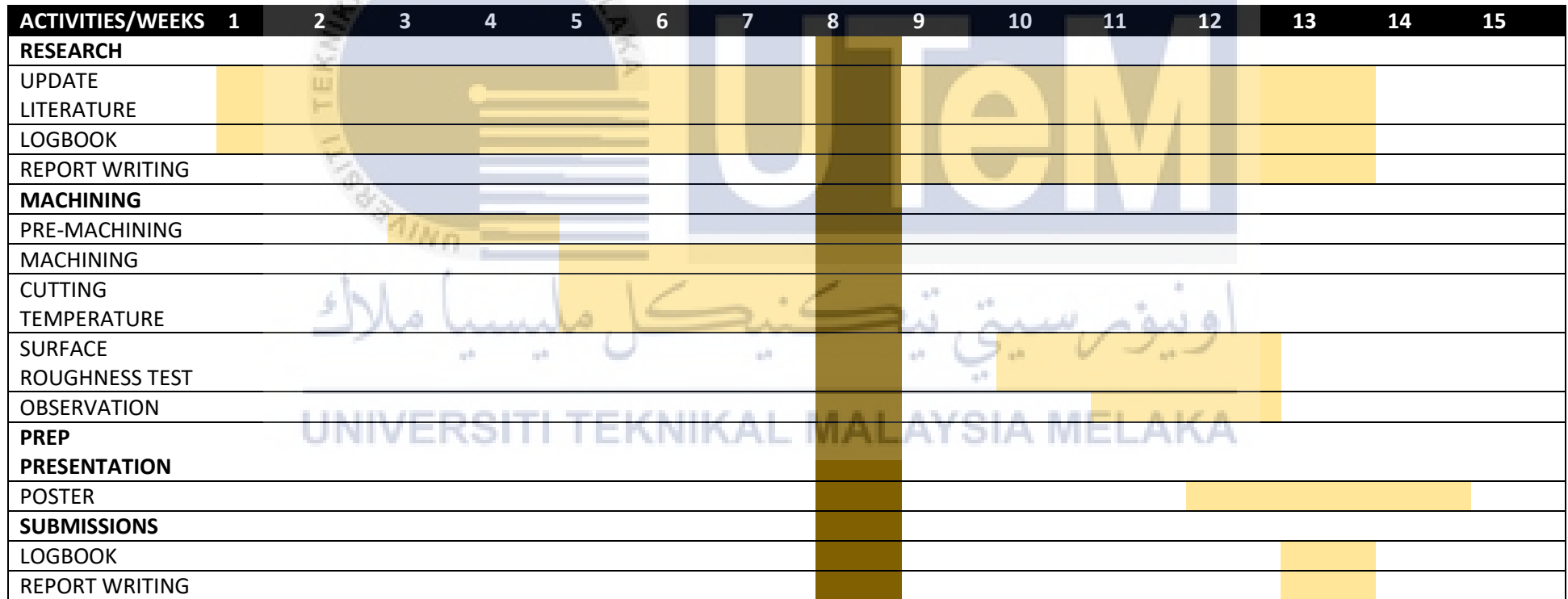
Appendix A Gantt chart PSM 1

PSM1



Appendix B Gantt chart PSM 2

PSM 2



References

- Abramovich, H. (2017). Stability and Vibrations of Thin-Walled Composite Structures. *Stability and Vibrations of Thin-Walled Composite Structures*, 1-47.
- Arquimedes Castillo-Morales, X. R.-F. (2021). Temperature Study during the Edge Trimming of Carbon Fiber-Reinforced Plastic [0]8/Ti6Al4V Stack Material. *Composite Science*.
- Azmi, A. (2013). Chip formation studies in machining fibre reinforced polymer composites. *Materials and Product Technology, Vol. 46*.
- Chunliang Kuo, J. L. (2021). The effects of cutting conditions and tool geometry on mechanics, tool wear and machined surface integrity when routing CFRP composites. *Journal of Manufacturing Processes* 64, 113-129.
- Deviprakash Jyothi Devan, F. A.-A. (2022). A study on tool wear of tungsten carbide cutters in edge trimming of CFRP. *Journal of Mechanical Science and Technology* 36 (5), pages2499–2510.
- Dhiraj Kumar, S. G. (2020). Machining damage and surface integrity evaluation during milling of UD-CFRP laminates: Dry vs. cryogenic. *Composite Structures* 247.
- Eshetu D. Eneyew, M. R. (2014). Experimental study of surface quality and damage when drilling unidirectional CFRP composites. *Journal of Material Research and Technology*, 354–362.
- Fu-Ji Wang, J.-B.-N.-X. (2020). Surface damage reduction of dry milling carbon fiber reinforced plastic/polymer using left–right edge milling tool. *Journal of Reinforced Plastics and Composites* 0(0), 1-13.
- Guangjian Bi, F. W. (2022). Wear characteristics of multi-tooth milling cutter in milling CFRP and its impact on machining performance. *Journal of Manufacturing Processes*, 580-593.
- Guoyi Hou, B. L. (2021). Investigation of high temperature effect on CFRP cutting mechanism based on a temperature controlled orthogonal cutting experiment. *Composite Structures* 268.
- Iker Urresti, I. L. (2022). Study of the surface integrity during CFRP trimming: Tool material and geometry, fiber orientation and tool wear effect analysis. *6th CIRP Conference on Surface Integrity* (pp. 660-664). Elsevier B.V.
- J. Sheikh-Ahmad, J. P. (2012). 5-Tool wear in machining processes for composites. *Machining Technology for Composite Materials*, 116-153.
- Marcelo André Santiago Barros, R. T. (2015). Advantages of applying composite material to replace metal alloys in aviation. *Journal of Engineering and Technology for Industrial Applications (JETIA) Vol.01*, 19-29.
- Mohd Azuwan Maoinser, F. A. (2014). Minimizing Drilling Thrust Force for HFRP Composite by Optimizing Process Parameters using Combination of ANOVA Approach and S/N Ratios Analysis. *MATEC Web of Conferences* 13, 04002. EDP Sciences.
- Petr Masek, P. Z. (2021). Cutting temperature measurement in turning of thermoplastic composites using a tool-work thermocouple. *The International Journal of Advanced Manufacturing Technology Volume 116*, 3163–3178.
- Priyansh Patel, V. C. (2018). Milling of Polymer Matrix Composites: A Review. *International Journal of Applied Engineering Research Volume 13*, 7455-7465.

- Rangasamy Prakash, V. K.-A. (2016). High-Speed Edge Trimming of CFRP and Online Monitoring of Performance of Router Tools Using Acoustic Emission. *Materials, Vol 9*.
- Robert Voss, L. S. (2017). Influence of fibre orientation, tool geometry and process parameters on surface quality in milling of CFRP. *CIRP Journal of Manufacturing Science and Technology*, 75-91.
- S. A. Sundi, R. I. (2021). Milling/Trimming of Carbon Fiber Reinforced Polymers (CFRP): Recent Advances in Tool Geometrical Design. *Machining and Machinability of Fibre Reinforced Polymer Composites*, 101-128.
- Saptarshi Maiti, M. R. (2022). Sustainable Fiber-Reinforced Composites: A Review. *Advanced Sustainable System, Vol 6*.
- Sheikh-Ahmad, J. Y. (2009). Chapter 2 Conventional Machining Operations. *Machining of Polymer Composites*, 1-315.
- T. D. Jagannatha, H. B. (2019). Optimization of machining parameters of hybrid fiber reinforced polymer composites using design of experiments. *AIP Conference Proceedings 2057, 020008*. AIP.
- Tan, C. A. (2015). Surface roughness analysis of carbon/glass hybrid polymer composites in drilling process based on Taguchi and response surface methodology. *Advanced Materials Research Vol. 1119*, 622-627.
- Tetsuya Tashiro, J. F. (2016). Cutting Characteristics in End-Milling of CFRP with Diamond-Coated Herringbone Tool. *International Journal of Automation Technology Vol.10 No.3*, 356-363.
- Yingjie Xu, J. Z. (2018). A review on the design of laminated composite structures: constant and variable stiffness design and topology optimization. *Advanced Composites and Hybrid Materials*, 460-477.
- ZAGHBANI, J.-F. C. (2011). Effect of Tool Geometry Special Features on Cutting Forces of Multilayered CFRP Laminates. *Recent advances in manufacturing engineering : proceedings of the 4th International Conference on Manufacturing Engineering, Quality and Production Systems (MEQAPS '11)*. WSEAS.

BORANG PENGESAHAN STATUS LAPORAN PROJEK SARJANA

TAJUK: Investigation On The Effect Of Tool Geometry Features To Minimize Damages During Trimming Of Hybrid Fibre Reinforced Polymer (HFRP) Material -Aero-Structural Component

SESI PENGAJIAN: 2023/2024 semester 1

Saya Nur Azalina binti Anuar

mengaku membenarkan tesis ini disimpan di Perpustakaan Universiti Teknikal Malaysia Melaka (UTeM) dengan syarat-syarat kegunaan seperti berikut:

1. Tesis adalah hak milik Universiti Teknikal Malaysia Melaka dan penulis.
2. Perpustakaan Universiti Teknikal Malaysia Melaka dibenarkan membuat salinan untuk tujuan pengajian sahaja dengan izin penulis.
3. Perpustakaan dibenarkan membuat salinan tesis ini sebagai bahan pertukaran antara institusi pengajian tinggi.
4. **Sila tandakan (✓)

- SULIT (Mengandungi maklumat yang berdarjah keselamatan atau kepentingan Malaysia sebagaimana yang termaktub dalam AKTA RAHSIA RASMI 1972)
- TERHAD (Mengandungi maklumat TERHAD yang telah ditentukan oleh organisasi/badan di mana penyelidikan dijalankan)
- TIDAK TERHAD

Disahkan oleh:

Nurazalina



Alamat Tetap:

Batu 9 Kampung Yooi Mukim Bohor,

07000 Langkawi, KEDAH

Cop Rasmi:

Ts. Dr. Syahrul Azwan bin Sundi @ Suandi,
Ketua Program Kedoktoran,
Fakulti Teknologi & Kejuruteraan Industri & Pembuatan (FTKIP),
Universiti Teknikal Malaysia Melaka

Tarikh: 12/01/2024

Tarikh: 19/01/2024

** Jika tesis ini SULIT atau TERHAD, sila lampirkan surat daripada pihak berkuasa/organisasi berkenaan dengan menyatakan sekali sebab dan tempoh laporan PSM ini perlu dikelaskan sebagai SULIT atau TERHAD.